

ABSTRACT

CHA, KI YOUNG. Mathematical Modeling of In Situ Chemical Oxidation with Permanganate -Model Development and Sensitivity Analyses. (Under the direction of Robert C. Borden.)

In situ chemical oxidation (ISCO) using permanganate can be a very effective technique for remediating groundwater and soil contaminated by chlorinated solvents. Injected reagent must be delivered to contaminated zone for successful clean up in ISCO. Many current remediation projects using chemical oxidation system are less effective than desired because of poor delivery of the chemical reagents to the treatment zone. A variety of site specific factors can affect reagent delivery including the amount of oxidant injected, volume of water injected, aquifer heterogeneity, and natural oxidant demand (NOD).

A model was developed and validated for simulating the transport and reaction of permanganate in the subsurface for ISCO. Six different kinetic relationships with zero, 1st, and 2nd order reaction were examined to identify the kinetic equation which best predicts the consumption of permanganate in experimental incubations. The numerical model RT3D was modified to simulate ISCO by developing a module that simulates reactions between permanganate, NOD and contaminants. The newly developed RT3D model was calibrated to an ISCO pilot test at MMR. The calibrated model provided an adequate match to the field data demonstrating this approach is appropriate for simulating ISCO of groundwater contaminants. A sensitivity analysis with validated model examined the influence of aquifer conditions and design variables on treatment efficiency.

Mathematical Modeling of In Situ Chemical Oxidation with Permanganate - Model Development and Sensitivity Analyses

by
Ki Young Cha

A thesis submitted to the Graduate Faculty of
North Carolina State University
in partial fulfillment of the
requirements for the Degree of
Master of Science

Civil Engineering

Raleigh, North Carolina

2008

APPROVED BY:

Dr. Mo. Gabr

Dr. G. Mahinthakumar

Dr. Robert C. Borden
Chair of Advisory Committee

BIOGRAPHY

Ki Young Cha is from Seoul, South Korea. He grew up in Seoul until his high school year. He attended the Handong University in Pohang, South Korea where he received a bachelor degree of Construction and Civil Engineering in 2005. During his college, he was a member of network security study group GHOST and basket ball club Air-Striker. At the last year of college, Ki Young was interested in groundwater remediation from one class introducing several groundwater treatment techniques. He started his Master of Science degree and under the guidance of Dr. Robert C. Borden at North Carolina State University. His research includes modeling of groundwater and contaminant transport and remediation in heterogeneous aquifers. Upon graduation he intends to pursue a Ph.D. program in Civil and Environmental Engineering under the guidance of Dr. Robert C. Borden.

ACKNOWLEDGEMENTS

First of all, I sincerely give this thesis to the LORD.

I would like to appreciate to my advisor, Dr. Robert Borden for all his guidance, support and patience during my Master of Science program. I really respect his humility, passion, insight, and knowledge for research. I also thank to my committee Dr. M. Gabr and Dr. G. Mahinthakumar for their time and efforts for the examination.

Very special thanks go to my wife, Miae Kwak, for consistent encouragement, endurance and pray. Her support allows me to finish my MS program. I would also like to thank my parents (Jongseok Cha, Haewon Choi) and brother for keep supporting and encouraging me through whole my life. I also thank to parent-in-law (Jongsub Kwak, Taesun Koo) and brother-in-law.

I would also like to thank NC State Korean Civil Engineering Association members and all other Korean friends. Lastly I thank everyone around me who have encouraged and helped me to study in peaceful and stable environment.

TABLE OF CONTENTS

| | |
|---|-------------|
| LIST OF TABLES ----- | vii |
| LIST OF FIGURES----- | viii |
| CHAPTER 1 INTRODUCTION ----- | 1 |
| 1.1 Contamination Problems----- | 1 |
| 1.2 Remediation Techniques----- | 1 |
| 1.3 In-Situ Chemical Oxidation (ISCO)----- | 2 |
| 1.4 Research Objectives ----- | 2 |
| CHAPTER 2 KINETICS OF PERMANGANATE CONSUMPTION BY AQUIFER MATERIAL ----- | 3 |
| 2.1 Introduction----- | 3 |
| 2.2 Fate and Transport of Permanganate in the Subsurface ----- | 3 |
| 2.2.1 Natural Oxidant Demand (NOD)----- | 4 |
| 2.2.2 Modeling Approaches----- | 6 |
| 2.3 Kinetic Model Evaluation ----- | 8 |
| 2.3.1 Model 1 – Zero Order Loss of MnO_4 ----- | 10 |
| 2.3.2 Model 2 – First Order Loss of MnO_4 ----- | 11 |
| 2.3.3 Model 3 – First Order Loss of NOD ----- | 13 |
| 2.3.4 Model 4 – Second Order Loss of MnO_4 and NOD----- | 14 |
| 2.3.5 Model 5 – Second Order Loss of MnO_4 with Fast and Slow NOD----- | 16 |
| 2.3.6 Model 6 – Second Order Loss of MnO_4 with Instantaneous and Slow NOD --- | 17 |
| 2.3.7 Kinetic Model Evaluation Summary----- | 19 |
| 2.4 MMR Best Fit Parameter ----- | 21 |
| CHAPTER 3 MODEL CALIBRATION AGAINST FIELD DATA FROM MMR PILOT TEST----- | 24 |

| | | |
|------------------|---|-----------|
| 3.1 | Introduction | 24 |
| 3.2 | Massachusetts Military Reservation (MMR) | 24 |
| 3.3 | Pilot Test | 27 |
| 3.4 | Modeling of MMR Pilot Test | 34 |
| 3.4.1 | Reaction Kinetics | 34 |
| 3.4.2 | Numerical Implementation | 35 |
| 3.4.3 | Model Setup | 36 |
| 3.4.3.1 | Grid and Initial Contaminant | 36 |
| 3.4.3.2 | Oxidant Injection | 39 |
| 3.4.3.3 | Reaction Parameters | 40 |
| 3.5 | Model Calibration | 42 |
| 3.5.1 | Simple Scoring Error Statistics (SSES) | 42 |
| 3.5.2 | Model Calibration Results | 42 |
| 3.6 | Conclusion | 46 |
| CHAPTER 4 | SENSITIVITY ANALYSIS | 47 |
| 4.1 | Introduction | 47 |
| 4.2 | Model Setup and Base Case Conditions | 47 |
| 4.2.1 | Scaling Factor | 51 |
| 4.2.2 | Typical Simulation Results | 52 |
| 4.2.3 | Criteria for Determining Contact Efficiency | 56 |
| 4.3 | Effect of Fluid Volume, Permanganate Mass and Time on Treatment Efficiency | 57 |
| 4.4 | Sensitivity Analyses | 61 |
| 4.4.1 | Effect of Slow NOD Reaction Rate on E_M | 64 |
| 4.4.2 | Effect of Total NOD on E_M | 64 |
| 4.4.3 | Effect of NOD_I on E_M | 66 |
| 4.4.4 | Effect of Initial Contaminant Concentration and Contaminant Retardation Factor on E_M | 67 |
| 4.4.5 | Effect of Aquifer Heterogeneity on E_M | 68 |
| CHAPTER 5 | SUMMARY AND CONCLUSIONS | 70 |

REFERENCES -----72

APPENDIX -----77

APPENDIX A MODEL VALIDATION -----78

 A.1 Analytical Solution -----78

 A.2 Model Setup -----79

 A.3 Comparison and Results -----80

LIST OF TABLES

| | | |
|-------------|---|----|
| Table 2-1 | Reported Values of NOD for Different Sites----- | 4 |
| Table 2-2 | Values of Total NOD and Reaction Rate Coefficients Reported by Jones (2007) ----- | 7 |
| Table 2-3 | Batch Experimental Conditions of Each Treatment ----- | 9 |
| Table 2-4 | Statistical Result of Model 1 Evaluation ----- | 11 |
| Table 2-5 | Statistical Result of Model 2 Evaluation ----- | 12 |
| Table 2-6 | Statistical Result of Model 3 Evaluation ----- | 13 |
| Table 2-7 | Statistical Result of Model 4 Evaluation ----- | 15 |
| Table 2-8 | Statistical Result of Model 5 Evaluation ----- | 16 |
| Table 2-9 | Statistical Result of Model 6 Evaluation ----- | 18 |
| Table 2-10 | Best Fit Coefficients for Model 4, 5, and 6 ----- | 20 |
| Table 2-11 | MMR Soil Sample Comparison ----- | 21 |
| Table 2-12a | Best Fit Parameter Estimates for MMR Soils – Initial NOD (mmol/g) ----- | 22 |
| Table 2-12b | Best Fit Parameter Estimates for MMR Soils – Slow Reaction Rate (k_{2S}) --- | 22 |
| Table 2-12c | Best Fit Parameter Estimates for MMR Soils – Fraction Instantaneous----- | 22 |
| Table 2-13 | Parameter Set for MMR ----- | 23 |
| Table 3-1 | Wells of Pilot Test----- | 31 |
| Table 3-2 | TCE Monitoring Results ----- | 32 |
| Table 3-3 | Permanganate Monitoring Results ----- | 33 |
| Table 3-4 | Injection Flow Rates and Concentrations Used in Model Simulations ----- | 40 |
| Table 3-5 | List of Common Parameters Used in Calibration Model ----- | 40 |
| Table 3-6 | The Details of 4 Different Scenarios ----- | 41 |
| Table 3-7a | Error Statistics between Simulated and Observed Contaminant (TCE) ----- | 43 |
| Table 3-7b | Error Statistics between Simulated and Observed Permanganate ----- | 43 |
| Table 3-8 | Error Statistics Comparing Simulated and Observed Permanganate Measurements with Increased Total NOD ----- | 46 |
| Table 4-1 | Base Case Simulation Conditions ----- | 49 |
| Table 4-2 | Characteristics for Low, Moderate, and High Levels of Heterogeneity ----- | 50 |
| Table 4-3 | Statistical Characteristics of Natural Log Transformed Hydraulic Conductivity Distributions used in Model Simulations----- | 50 |
| Table 4-4 | Input Parameters used in Sensitivity Analyses Simulations----- | 63 |
| Table A-1 | Parameters for Analytical Solution ----- | 79 |
| Table A-2 | Parameters for Numerical Analysis----- | 79 |

LIST OF FIGURES

| | |
|---|----|
| Figure 2-1 Comparison of Observed Values of ΔMnO_4 with Model 1 Simulation Results (all data for Soil C) ----- | 11 |
| Figure 2-2 Comparison of Observed Values of ΔMnO_4 with Model 2 Simulation Results (all data for Soil C) ----- | 12 |
| Figure 2-3 Comparison of Observed Values of ΔMnO_4 with Model 3 Simulation Results (all data for Soil C) ----- | 14 |
| Figure 2-4 Comparison of Observed Values of ΔMnO_4 with Model 4 Simulation Results (all data for Soil C) ----- | 15 |
| Figure 2-5 Comparison of Observed Values of ΔMnO_4 with Model 5 Simulation Results (all data for Soil C) ----- | 17 |
| Figure 2-6 Comparison of Observed Values of ΔMnO_4 with Model 6 Simulation Results (all data for Soil C) ----- | 19 |
| Figure 3-1 Location of MMR on Cape Cod, Massachusetts ----- | 25 |
| Figure 3-2 Map of Plume Distribution of MMR (grey area represent MMR, red line represent plume boundary, AFCEE 2007b)----- | 26 |
| Figure 3-3 Map of CS-10 Plume (grey area represent MMR, red line represent plume boundary, AFCEE 2007b)----- | 27 |
| Figure 3-4 Map of Cross Section of Pilot Test Area (CH2MHILL 2007) ----- | 29 |
| Figure 3-5 Plan View of MMR Pilot Test Simulation Grid----- | 36 |
| Figure 3-6 Profile View of MMR Pilot Test Simulation Grid----- | 37 |
| Figure 3-7 Cross-Section View of Permeability Distribution (deep red color indicates high permeability and white color indicates low permeability area) ----- | 37 |
| Figure 3-8 Plan View of 15 th Layer of Model with Contaminants Distribution and Injection and Monitoring Wells ----- | 38 |
| Figure 3-9 Front View of 50 th Row of Model with Contaminants Distribution and Injection and Monitoring Wells (thick bar indicate injection well, blue box indicate well screen and triangle indicate monitoring well) ----- | 39 |

| | |
|--|----|
| Figure 3-10a Profile View of Contaminant Distribution at 6, 18, 30 and 90 Days of Simulation with Scenario 4 (deep red indicate high concentration of contaminant)----- | 44 |
| Figure 3-10b Profile View of Permanganate Distribution at 6, 18, 30 and 90 Days of Simulation with Scenario 4 (deep red indicate high concentration of permanganate)----- | 45 |
| Figure 4-1 Hypothetical Injection Grid Showing Model Domain Subarea----- | 48 |
| Figure 4-2 Model Domain for Numerical Simulations ----- | 49 |
| Figure 4-3 Horizontal Hydraulic Conductivity, Permanganate (M), NOD_I , NOD_S and Contaminant Distribution (C) in Top Layer of Aquifer (see Figure 4-4) (with moderately heterogeneous aquifer (realization #3), wells 1-5 are injected with $SF_V = SF_M = 0.25$)----- | 53 |
| Figure 4-4 Vertical Hydraulic Conductivity, Permanganate (M), NOD_I , NOD_S and Contaminant Distribution (C) in Last Row of Aquifer (bottom row of Figure 4-3) (with moderately heterogeneous aquifer (realization #1), wells 1-5 are injected with $SF_V = SF_M = 0.25$) ----- | 55 |
| Figure 4-5a Variation in Aquifer Volume Contact Efficiency (E_V) with Time where Fluid Injection Volume is held Constant ($SF_V=0.25$) and Permanganate Mass Varies (SF_M varies from 0.05 to 1.0)) ----- | 57 |
| Figure 4-5b Variation in Contaminant Mass Treatment Efficiency (E_M) with Time where Fluid Injection Volume is held Constant ($SF_V=0.25$) and Permanganate Mass Varies (SF_M varies from 0.05 to 1.0)) ----- | 58 |
| Figure 4-6a Variation in Aquifer Volume Contact Efficiency (E_V) with Time where Permanganate Concentration is held Constant ($SF_V=Sf_M$) and the Volume of the Permanganate Injection Solution Varies (both SF_V and SF_M varies from 0.05 to 1.0)----- | 59 |
| Figure 4-6b Variation in Contaminant Mass Treatment Efficiency (E_M) with Time where Permanganate Concentration is held Constant ($SF_V=Sf_M$) and the Volume of | |

| | | |
|-------------|---|----|
| | the Permanganate Injection Solution Varies (both SF_V and SF_M varies from 0.05 to 1.0)----- | 60 |
| Figure 4-7 | Variation in Contaminant Mass Treatment Efficiency (E_M) at 180 days after Injection with Mass and Volume Scaling Factors ----- | 61 |
| Figure 4-8 | Effect of Slow NOD Reaction Rate (k_{2S}) on E_M at 180 days ($SF_V=S F_M$) ----- | 64 |
| Figure 4-9 | Effect of Total NOD on E_M at 180 days ($SF_V=S F_M$) ----- | 65 |
| Figure 4-10 | Effect of Slow NOD Reaction Rate (k_{2S}) and Total NOD on E_M at 180 days ($SF_V = S F_M$) ----- | 66 |
| Figure 4-11 | Effect of Fraction NOD_I on E_M at 180 days ($SF_V = S F_M$)----- | 67 |
| Figure 4-12 | Effect of Initial Contaminant Concentration on E_M at 180 days ($SF_V = S F_M$) -- | 68 |
| Figure 4-13 | Effect of Retardation Factor on E_M at 180 days ($SF_V = S F_M$) ----- | 68 |
| Figure 4-14 | Effect of Aquifer Heterogeneity on E_M at 180 days ($SF_V = S F_M$) (error bars show the standard deviation in E_M observed in five permeability realizations for each level of heterogeneity)----- | 69 |
| Figure A-1 | Comparison of Analytical Solution and Numerical Modeling Result with Non-Reactive at 9.9m of Model. ----- | 80 |
| Figure A-2 | Comparison of Analytical Solution and Numerical Modeling Result with Reactive at 9.9m of Model. ----- | 81 |

CHAPTER 1 INTRODUCTION

1.1 Contamination Problems

Ground water contamination can result from a variety of human activities including chemical use for industry, fertilizer in agriculture, leachate from landfills, leaking underground storage tanks and septic systems. In the US, groundwater is the source of over 20 percent of water used for household, industry or agriculture, and contaminated groundwater could be serious threat to human health (Hutson 2004). Many of researchers are actively studying groundwater remediation techniques.

Many organic contaminants have low water solubility and are resistant to biodegradation (WSTC 2004). Tetrachloroethylene (PCE) is one of the most common ground water contaminants, and has been used for dry-cleaning, textile processing, metal cleaning and vapor degreasing for several decades. PCE has been detected at 60% of the National Priority List sites (ATSDR 2004, 2007).

1.2 Remediation Techniques

A variety of remediation techniques have been developed to treat organic contaminants in groundwater. Treatment technologies for source control and groundwater plume control include two of major categories: (1) ex-situ technologies and (2) in-situ technologies. Cumulative data from 1982 to 2005 show that ex-situ techniques were used more commonly for source control and groundwater treatment than in-situ. However, the fraction of sites where groundwater is treated by in-situ techniques is growing. Between 2002 and 2005, in situ remediation methods have been used for source control at more than half of the reported sites (US EPA 2007).

1.3 In-Situ Chemical Oxidation (ISCO)

In-situ chemical oxidation (ISCO) can be a very effective technique for destroying subsurface contaminants. During ISCO, a chemical oxidant is injected into the subsurface to convert hazardous contaminants to less harmful compounds. Several different oxidants are capable of degrading common contaminants including permanganate (MnO_4^-), hydrogen peroxide (H_2O_2), persulfate ($\text{S}_2\text{O}_8^{2-}$) and ozone (O_3). However for ISCO to be effective, injected reagents must contact the contaminants. A variety of site specific factors affect the efficiency of contact between reagents and contaminants including the amount of oxidant injected, volume of water injected, aquifer heterogeneity, natural oxidant demand (NOD), and soil type (US EPA 1998; Huling 2006).

1.4 Research Objectives

The overall objective of this research is develop a modeling approach to assist engineers in designing systems for distributing chemical oxidants dissolved in water for in situ chemical oxidation of groundwater contaminants. Currently, chemical oxidation systems are being used to clean up contaminated groundwater and soil at many private and DoD sites. However at too many sites, the remediation process does not meet cleanup objectives. The most common problem is poor delivery of the chemical reagents to the treatment zone. Treatment efficiency could be improved and costs reduced, if engineers had a simple and effective tool for design of ISCO systems.

The objective of this research is to develop and validate a model for simulating the transport of permanganate in the subsurface of ISCO. Once validated, this model will be used to conduct a series of sensitivity analyses to identify those variables that have the greatest influence on contact efficiency and treatment.

CHAPTER 2 KINETICS OF PERMANGANATE CONSUMPTION BY AQUIFER MATERIAL

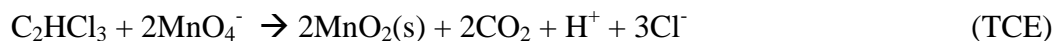
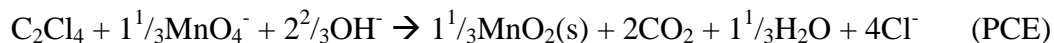
2.1 Introduction

When permanganate is injected into the subsurface, a portion of the material reacts with the target contaminant and a portion reacts with the aquifer material. The amount of permanganate that reacts with non-target chemicals is often referred to as the natural oxidant demand (NOD). When estimating the required amount of reagent to inject, we need to account for both permanganate consumed by the target chemicals and the NOD. If the NOD is not considered, the permanganate will be depleted more rapidly than expected and treatment efficiency may be less than desired.

2.2 Fate and Transport of Permanganate in the Subsurface

Permanganate has been used for wastewater and drinking water treatment for many years (Steel and McGhee 1979; Eilbeck and Mattock 1987). In contrast, permanganate has been used for groundwater remediation for less than 20 years. However, recent work has shown permanganate to be an effective oxidant for treatment of chlorinated solvents (perchloroethene (PCE) and trichloroethene (TCE)) and aromatic hydrocarbons (naphthalene, phenanthrene, pyrene and phenols) (Vella et al. 1990; Leung et al. 1992; Vella and Veronda 1992; Gates et al. 1995, 2001; Yan and Schwartz 1996; 1999; Schnarr et al. 1998; West et al. 1998; Siegrist et al. 1998a, b, 2000, 2001; Lowe et al. 1999).

Representative reactions illustrating the oxidation of PCE (C_2Cl_4) and TCE (C_2HCl_3) by permanganate are shown below.



Based on this stoichiometry, 1.81 g of permanganate is needed to degrade 1 g of TCE, releasing 1.32 g of manganese dioxide, 0.67 g of carbon dioxide and 0.81 g of Cl- (Siegrist et al. 2001).

2.2.1 Natural Oxidant Demand (NOD)

In many cases, the natural oxidant demand (NOD) controls the amount of reagent which must be injected for effective treatment (Marvin et al. 2002). NOD is exerted when permanganate reacts with a variety of naturally occurring materials including ferrous iron, sulfides and natural organic carbon. NOD is commonly measured by reacting aquifer material with a permanganate solution and measuring change in permanganate concentration over time. Currently, there is no standard procedure for measuring NOD and experimental conditions (amount of sediment, permanganate concentration, and reaction time) often vary between different investigators. However, efforts are underway to develop a more standardized approach (ASTM 2007). NOD is typically reported as mass of permanganate consumed per unit mass of aquifer solids (Siegrist et al. 2000; Marvin et al. 2002).

Table 2-1 shows the measured values of NOD value for several different sites and experimental conditions. Reported NOD values range from 0.3 to 88 g MnO₄ / Kg indicating NOD can vary dramatically between sites.

Table 2-1 Reported Values of NOD for Different Sites

| Source | NOD | | Site | Description |
|------------------------|-----------|-----------|-----------------------------|--------------------------------------|
| | g/Kg | mmol/Kg | | |
| Mumford et al. 2005 | 1.2 | 10 | Canadian Forces Base Borden | Batch test |
| | 0.35 | 3 | | Column test |
| Mumford et al. 2004 | 0.51-0.75 | 4.29-6.3 | Canadian Forces Base Borden | Push-pull test Static |
| | 0.29-0.42 | 2.44-3.53 | | Push-pull test, Drift or Reaction |

Table 2-1 Continued

| | | | | |
|--------------------------|-------|---------|--|--------------------------------|
| Urynowicz 2008 | 2.9 | 24 | - | Low dose, 48 hr |
| | 4.8 | 40 | - | Mid dose, 48 hr |
| | 6.1 | 51 | - | High dose, 48 hr |
| | 23.2 | 195 | - | High dose, 6 weeks |
| Oberle et al., 2000 | 0.2 | 1.68 | Northern Ohio | Saturated Sand |
| | 15-20 | 126-168 | From MI | Unsaturated Sandy Clay |
| Chambers et al., 2000 | 7.61 | 64 | From CA | Silt, 14 days |
| | 7.16 | 60 | | Clay, 14 days |
| | 4.49 | 38 | | Sand, 14 days |
| Drescher et al. 1998 | 30 | 252 | - | - |
| Siegrist et al. 2001 | 11 | 92 | - | - |
| Hood 2000a | 1 | 8 | Canadian Forces Base Borden | - |
| Xu 2006 | 2.12 | 17.82 | Groundwater Field Laboratory, CFB Borden, Ontario | fine/medium sand |
| | 2.28 | 19.16 | National Test Site, Dover AFB, DE | sandy loam |
| | 32.29 | 27.134 | East Gate Disposal Yard, Fort, Lewis, WA | loamy sand, gravel, cobbles |
| | 0.77 | 6.47 | Milan Army Ammunition Plant, TN | Sand |
| | 11.42 | 95.97 | Launch Complex 34, Cape Canaveral AFS, FL | loamy coarse/medium sand |
| | 5.5 | 46.22 | | |
| | 87.87 | 738.4 | NFF, Cecil Field, FL | loamy fine sand |
| | 2.54 | 21.34 | NIROP, Bacchus Works Facility, Utah | gravels, loam |

2.2.2 Modeling Approaches

Several investigators (Yan and Schwartz 1999; Siegrist et al., 2001; Mumford et al., 2002, 2005; Haselow et al., 2003; Urynowicz et al., 2008;) have reported that the measured NOD varies with the MnO_4 concentration (dose) and reaction time. Higher doses of MnO_4 commonly result in higher measured values of NOD (Siegrist 2001; Haselow et al 2003; Mumford 2004). The rate of permanganate consumption by NOD is also reported to vary with time, where MnO_4 concentrations tend to decrease rapidly within the first 48 hours and more slowly thereafter (ASTM 2007).

A number of different modeling approaches have been applied to simulate ISCO treatment with permanganate (Hood and Thomson, 2000; Reitsma and Dai, 2001; Mumford, 2002; Xu, 2006; Jones, 2007). Ignoring the effect of NOD on permanganate transport could result in an over estimate of treatment efficiency. In contrast, assuming an instantaneous reaction between permanganate and NOD can over estimate the actual NOD exerted. The most common modeling approach employed (Zhang and Schwartz 2000, Xu 2006, and Jones 2007) simulates the reaction between permanganate (M) and NOD (N) as a 2nd order reaction where,

$$dM/dt = -k_2 M N$$

However, a simple 2nd order approach may not adequately represent the rapid consumption of MnO_4 , often observed during the first 24 hours of NOD tests.

Jones (2007) developed a 2nd order NOD model which included both fast and slow reaction sites. The objective of this work was to develop a general kinetic model that could accurately represent the experimental batch and column results generated by Xu (2006). Batch test results showed that the permanganate consumption rate is determined by initial permanganate concentration and the consumption rate decreased over the course of experiment. Large amounts of oxidizable organic matter (OAM) were consumed during the first 5 minutes and then OAM decreased more slowly over the next 1 to 2 hours. Subsequent column tests confirmed the fast and slow reaction kinetics. The equations developed by Jones for simulating NOD kinetics in the batch and column tests are shown below.

$$\frac{dC_{OAM}^{fast}}{dt} = -k_{OAM}^{fast} (C_{OAM}^{fast})^{\alpha_{fast}} (C_{MnO_4^-})^{\beta_{fast}}$$

$$\frac{dC_{OAM}^{slow}}{dt} = -k_{OAM}^{slow} (C_{OAM}^{slow})^{\alpha_{slow}} (C_{MnO_4^-})^{\beta_{slow}}$$

and,

$$\frac{dC_{MnO_4^-}}{dt} = -k_{MnO_4^-}^{fast} (C_{OAM}^{fast})^{\alpha_{fast}} (C_{MnO_4^-})^{\beta_{fast}} - k_{MnO_4^-}^{slow} (C_{OAM}^{slow})^{\alpha_{slow}} (C_{MnO_4^-})^{\beta_{slow}}$$

The slow OAM reaction rate was estimated assuming the reaction was first order with respect to both OAM and permanganate concentration ($\alpha_{slow} = \beta_{slow} = 1$). **Table 2-2** shows estimated values of the slow reaction rate coefficients converted from L g OAM⁻¹ min⁻¹ to L mmol MnO₄⁻¹ day⁻¹ for different initial KMnO₄ concentrations. The slow NOD reaction rate varied from 0.014 to 0.72 L/mmol-day with a median value of 0.077 L/mmol-day.

Table 2-2 Values of Total NOD and Reaction Rate Coefficients Reported by Jones (2007)

| Site | Total NOD | Initial KMnO ₄ Conc. | 2nd Order Slow NOD reaction Rate |
|--------|-----------|---------------------------------|----------------------------------|
| | mmol/Kg | g KMnO ₄ /L | L/mmol-day |
| Borden | 17.8 | 0.1 | 0.721 |
| | | 0.2 | 0.181 |
| | | 0.3 | 0.077 |
| | | 0.4 | 0.038 |
| | | 0.5 | 0.054 |
| EGDY | 271.3 | 0.5 | 0.404 |
| | | 1.0 | 0.247 |
| | | 1.5 | 0.118 |
| | | 2.0 | 0.078 |
| | | 2.5 | 0.057 |

Table 2-2 Continued

| | | | |
|----------|------|------|-------|
| LC34-LSU | 96.0 | 0.4 | 0.180 |
| | | 0.6 | 0.087 |
| | | 0.8 | 0.046 |
| | | 1.0 | 0.027 |
| | | 1.2 | 0.016 |
| LC34-USU | 46.2 | 0.06 | 0.579 |
| | | 0.2 | 0.102 |
| | | 0.4 | 0.036 |
| | | 0.6 | 0.028 |
| | | 0.8 | 0.014 |

2.3 Kinetic Model Evaluation

At present, there is no common consensus on the best approach for simulating MnO_4 consumption by NOD. However, there does seem to be some agreement that: 1) NOD is often composed of different components or fractions; 2) some components react fairly quickly (minutes to hours); 3) some components react more slowly (days to months); and 4) the effective NOD is a function of permanganate concentration with higher concentrations resulting in higher effective NOD.

In this project, we will be using groundwater flow, transport and reaction models (MODFLOW and RT3D) to evaluate the effect of injection conditions on treatment efficiency in a three dimensional (3-D) heterogeneous aquifer. The model must adequately represent the kinetics of MnO_4 consumption by NOD, but must be relatively simple to implement and not result in an excessive computational burden. Given that there is no one modeling approach that is generally accepted, we chose to evaluate six different approaches for describing NOD kinetics. Each of the modeling approaches was calibrated to match the results of all batch NOD incubations with a sample of aquifer material (Soil C) from the Massachusetts Military Reservation (MMR). Experimental data was provided by Dr. Michelle Crimi of Clarkson University. The model performance was then evaluated based on a visual comparison

of measured and simulated NOD, and statistical measures describing the goodness of fit. The batch incubations were conducted in glass jars with varying amounts of aquifer material and KMnO_4 (500, 1000 and 5000 mg/L), aquifer material (16, 32 and 48 g) and water (10, 20 and 30 g) (see **Table 2-3** for the different treatments). In addition, three different mixing conditions were evaluated: (1) complete mixing; (2) mixing once per day; and (3) static (mix only before sample collection). MnO_4 concentration was typically measured approximately 16 times over the 28 day incubation period resulting in a total of 834 MnO_4 measurements.

Table 2-3 Batch Experimental Conditions of Each Treatment

| Treatment | KMnO_4 Conc. (init mg/L) | mass solids (g) | mass water (g) |
|------------------|---|------------------------|-----------------------|
| 1 | 5000 | 16 | 30 |
| 2 | 1000 | 16 | 30 |
| 3 | 500 | 16 | 30 |
| 4 | 5000 | 32 | 20 |
| 5 | 1000 | 32 | 20 |
| 6 | 500 | 32 | 20 |
| 7 | 5000 | 48 | 10 |
| 8 | 1000 | 48 | 10 |
| 9 | 500 | 48 | 10 |

The kinetic models evaluated in this work are summarized below. Each model was coded into MS Excel as a Visual BASIC subroutine using a 4th order Runge-Kutta solution of the ordinary differential equations (ODE's). An initial set of model coefficients was assumed, and used to predict the variation in MnO_4 concentrations vs. time for all incubations of Soil C. The goodness of fit was then evaluated as the root mean square error (RMSE) between simulated and measured MnO_4 concentration in all incubations of Soil C. Best fit parameter values were found using the Solver function in Excel to search for the parameter set that resulted in the smallest RMSE. Best fit parameter values were obtained for the three soils for

each mixing condition (complete mix, mix once per day, and static) and a fourth condition where all the data for the soil was pooled together, ignoring mixing condition.

For each of the models, the ME (Mean Error) and the RSME are presented as indicators of goodness of fit. The best model should have a value of ME and RMSE close to zero. Graphs are also presented showing the measured change in MnO_4 concentration from the start of the incubation (ΔMnO_4) vs. simulated ΔMnO_4 with the pooled data for Soil C. Ideally, the experimental measurements should cluster around the 45° line indicating a 1:1 match between measured and simulated values. Clustering of data away from the 45° line indicates that there is some trend in the experimental results that is not captured by the kinetic model.

In each of the models presented below, M is the MnO_4 concentration (mol L^{-1}), ρ_B is the soil bulk density (Kg L^{-1}) and n is porosity (dimensionless).

2.3.1 Model 1 – Zero Order Loss of MnO_4

Model 1 assumes that MnO_4 concentration declines at a constant (zero order) rate with time, independent of the amount of NOD. This very simplified approach was included to provide a comparison with more complex kinetic representations. The change in permanganate concentration (M) is represented by the equation 2-1.

$$\frac{dM}{dt} = -k_0 \quad (2-1)$$

where,

$$k_0 = \text{zero order } \text{MnO}_4 \text{ consumption rate (mmol L}^{-1} \text{ d}^{-1}\text{)}$$

Experimental results are compared to simulated values for Model 1 in **Figure 2-1** and **Table 2-4**. As expected, Model 1 provided a relatively poor fit to the experimental data. Visual examination of the results shown in **Figure 2-1** show that simulated values of ΔMnO_4 are clustered near the x-axis and do not increase with increasing values of measured ΔMnO_4 .

Table 2-4 Statistical Result of Model 1 Evaluation

| Mixing Condition | k_0 | Mean Error | RMSE |
|------------------------|------------|------------|------|
| | mmol/L-day | | |
| Complete condition | 0.143 | -0.99 | 1.42 |
| Once per day condition | 0.117 | -1.00 | 1.50 |
| Static condition | 0.110 | -0.64 | 1.00 |
| Total condition | 0.120 | -0.88 | 1.31 |

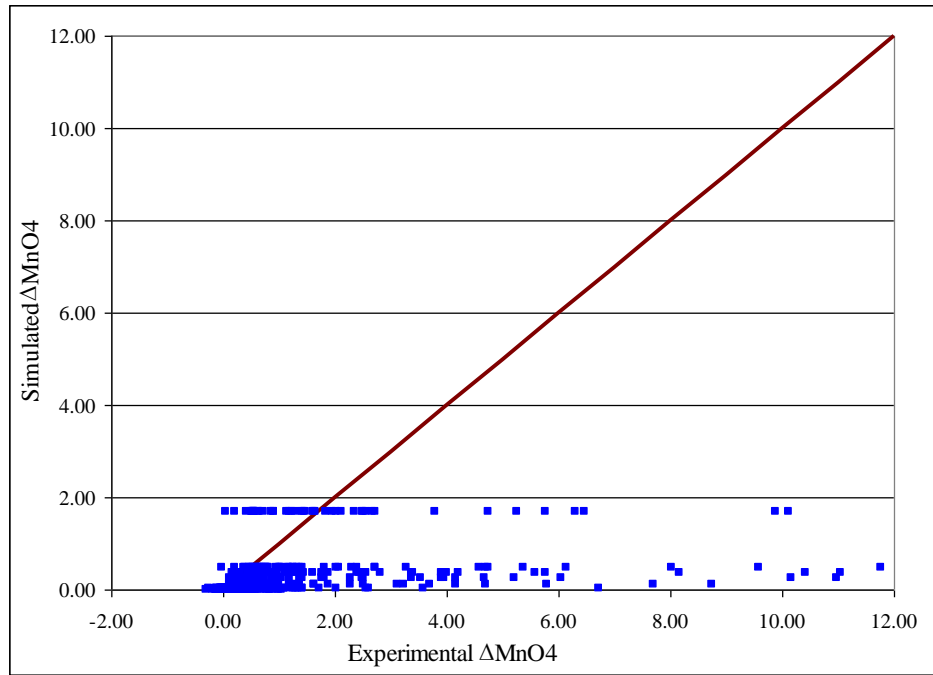


Figure 2-1 Comparison of Observed Values of ΔMnO_4 with Model 1 Simulation Results (all data for Soil C)

2.3.2 Model 2 – First Order Loss of MnO_4

Model 2 assumes that MnO_4 concentration declines at a first order rate with time, independent of the amount of NOD. The change in permanganate concentration (M) is represented by the equation 2-2.

$$\frac{dM}{dt} = -k_{1M}M \quad (2-2)$$

where,

$k_{IM} = 1^{\text{st}}$ order MnO_4 consumption rate (d^{-1})

Experimental results are compared to simulated values for Model 2 in **Figure 2-2** and **Table 2-5**. Model 2 provided a slightly better fit to the data than Model 1. However, the fit was still relatively poor. One difference is that Model 2 predicted higher values of ΔMnO_4 for higher initial MnO_4 concentrations. This resulted in a small improvement in the goodness of fit statistics.

Table 2-5 Statistical Result of Model 2 Evaluation

| Mixing Condition | k_1 | Mean Error | RMSE |
|------------------------|--------|------------|------|
| | 1/day | | |
| Complete condition | 0.0120 | -0.86 | 1.34 |
| Once per day condition | 0.0123 | -0.79 | 1.33 |
| Static condition | 0.0122 | -0.42 | 0.87 |
| Total condition | 0.0121 | -0.69 | 1.18 |

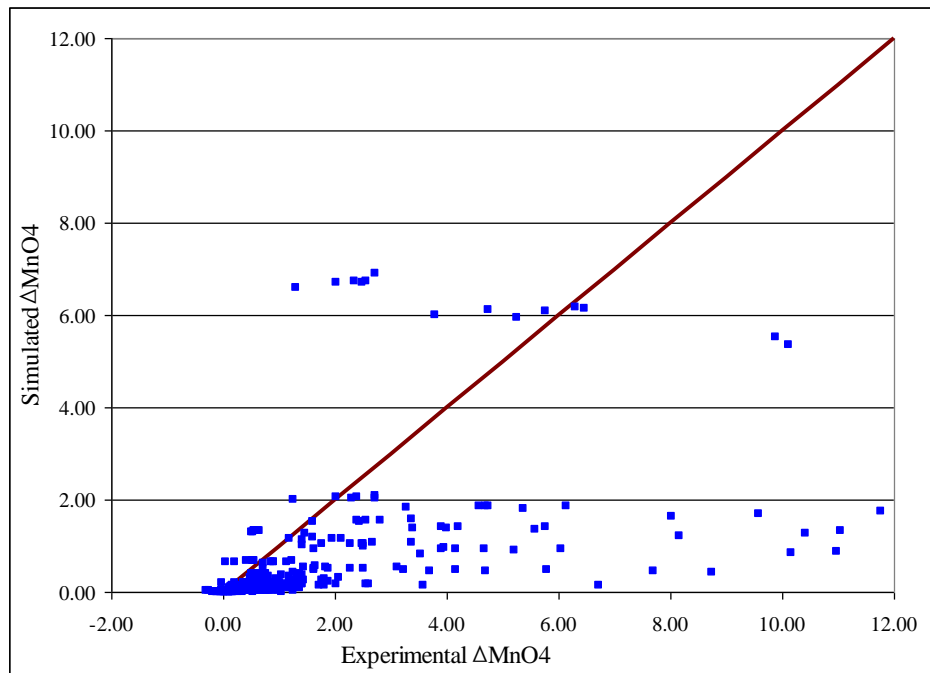


Figure 2-2 Comparison of Observed Values of ΔMnO_4 with Model 2 Simulation Results (all data for Soil C)

2.3.3 Model 3 – First Order Loss of NOD

Model 3 assumes that NOD concentration declines at a first order rate with time, and the change in MnO_4 concentration is equal to the change in NOD. This very simple approach was included to provide a comparison with more complex kinetic representations. The change in permanganate concentration (M) is represented by the equations 2-3a and 2-3b.

$$\frac{dN_F}{dt} = -k_{1N} N \quad (2-3a)$$

$$\frac{dM}{dt} = -\rho_B k_{1N} N / n \quad (2-3b)$$

where,

$$k_{1N} = 1^{\text{st}} \text{ order NOD consumption rate (d}^{-1}\text{)}$$

Experimental results are compared to simulated values for Model 3 in **Figure 2-3** and **Table 2-6**. Model 3 provided a significantly better fit to the data than Models 1 and 2. However, visual examination of **Figure 2-3** shows that the fit is still less than desired. There appears to be clusters of data above and below the 45° line, indicating there is one group of measurements where Model 3 consistently under predicts the observed ΔMnO_4 , and a second group of data where while Model 3 consistently over predicts the observed ΔMnO_4 .

Table 2-6 Statistical Result of Model 3 Evaluation

| Mixing Condition | k_{1N} | NOD initial | Mean Error | RMSE |
|------------------------|----------|-------------|------------|------|
| | 1/day | mmol/g | | |
| Complete condition | 1.78 | 0.00096 | -0.380 | 1.14 |
| Once per day condition | 0.71 | 0.00060 | -0.791 | 1.27 |
| Static condition | 0.25 | 0.00093 | -0.422 | 0.94 |
| Total condition | 0.51 | 0.00081 | -0.596 | 1.15 |

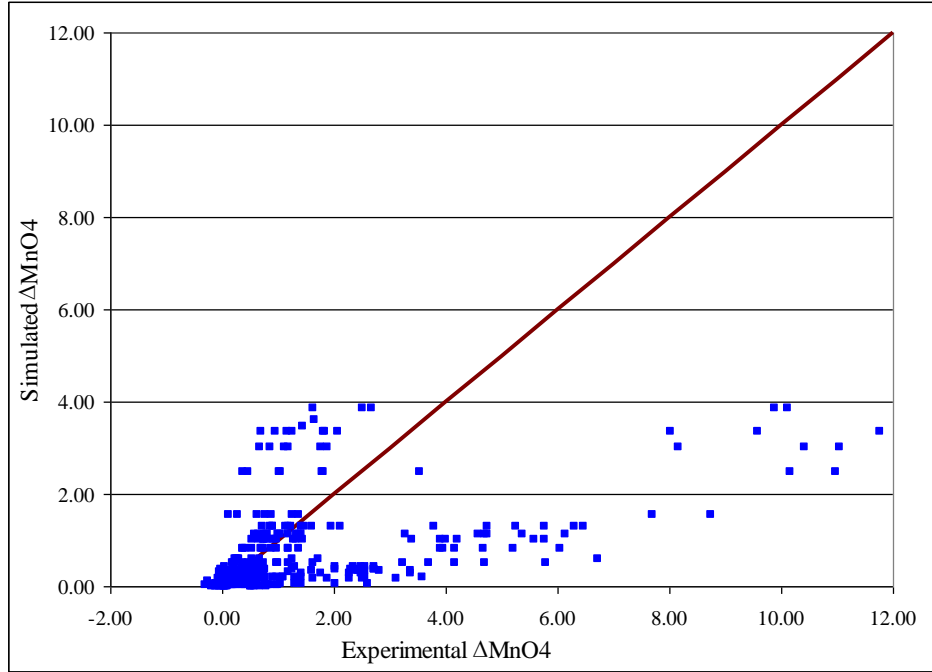


Figure 2-3 Comparison of Observed Values of ΔMnO_4 with Model 3 Simulation Results (all data for Soil C)

2.3.4 Model 4 – Second Order Loss of MnO_4 and NOD

Model 4 assumes that the concentrations of MnO_4 and NOD both decline as a first order function of both MnO_4 and NOD (overall second order function). This approach has been used by a number of investigators including Zhang and Schwartz (2000) and Xu (2006). Changes in permanganate concentration (M) and NOD concentration (N) are represented by the equations 2-4a and 2-4b.

$$\frac{dM}{dt} = -\rho_B k_2 NM / n \quad (2-4a)$$

$$\frac{dN}{dt} = -k_2 NM \quad (2-4b)$$

where,

$$k_2 = 2^{\text{nd}} \text{ order NOD consumption rate (L mmol}^{-1} \text{ d}^{-1}\text{)}$$

Experimental results are compared to simulated values for Model 4 in **Figure 2-4** and **Table 2-7**. Model 4 provided a significantly lower RMSE compared to

Model 3 indicating a significant improvement in model fit. However, values of ME indicate a slightly poorer fit. However, there is no obvious clustering of the data, indicating there are no consistent trends that are not captured by the model.

Table 2-7 Statistical Result of Model 4 Evaluation

| Mixing Condition | k_2 | NOD initial | Mean Error | RMSE |
|------------------------|------------|-------------|------------|------|
| | L/mmol-day | mmol/g | | |
| Complete condition | 0.0317 | 0.00226 | -0.15 | 0.73 |
| Once per day condition | 0.0152 | 0.00308 | -0.12 | 0.73 |
| Static condition | 0.0072 | 0.00277 | -0.20 | 0.53 |
| Total condition | 0.0128 | 0.00286 | -0.18 | 0.72 |

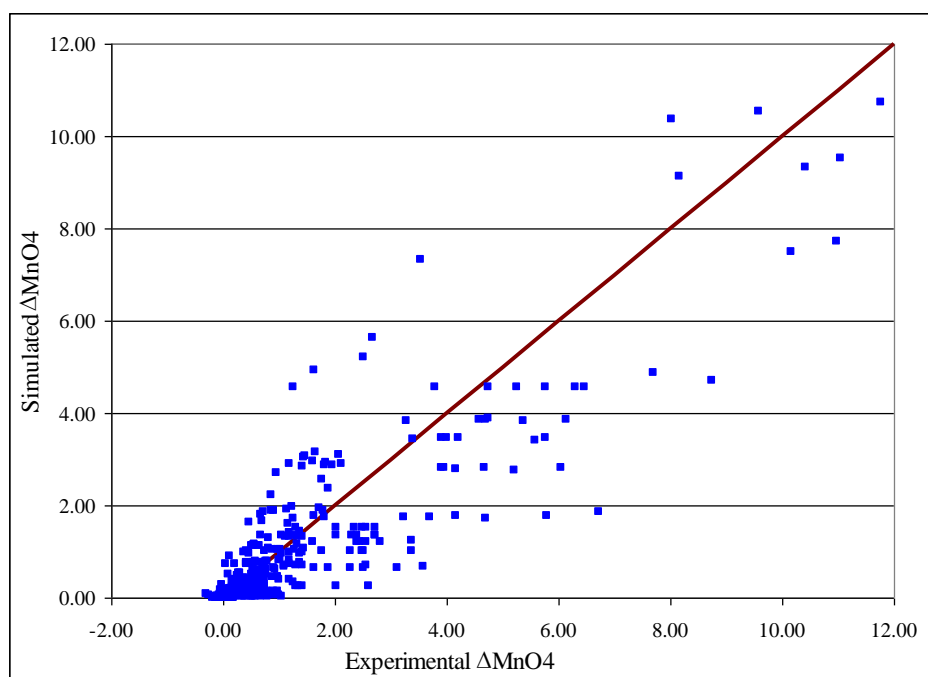


Figure 2-4 Comparison of Observed Values of ΔMnO_4 with Model 4 Simulation Results (all data for Soil C)

2.3.5 Model 5 – Second Order Loss of MnO₄ with Fast and Slow NOD

Model 5 is similar to Model 4. However, the NOD is assumed to be composed of a fast fraction and a slow fraction, similar to the modeling approach employed by Jones (2007). The change in permanganate (M), fast NOD (N_F), and slow NOD (N_S) are represented by equations 2-5a, b and c.

$$\frac{dM}{dt} = -\rho_B k_{2F} N_F M / n - \rho_B k_{2S} N_S M / n \quad (2-5a)$$

$$\frac{dN_F}{dt} = -k_{2F} N_F M \quad (2-5b)$$

$$\frac{dN_S}{dt} = -k_{2S} N_S M \quad (2-5c)$$

where,

k_{2F} = 2nd order Fast NOD consumption rate (L mmol⁻¹ d⁻¹)

k_{2S} = 2nd order Slow NOD consumption rate (L mmol⁻¹ d⁻¹)

Experimental results are compared to simulated values for Model 5 in **Figure 2-5** and **Table 2-8**. Error statistics for Model 5 were very similar to Model 4 indicating that separation of the NOD into a fast and slow fraction did not significantly improve the model fit for the MMR soils. However, Model 5 run times were significantly longer than for Model 4. This was because the high reaction rates for fast NOD required a shorter computational time step.

Table 2-8 Statistical Result of Model 5 Evaluation

| Mixing Condition | k_{2F} | k_{2S} | Fraction Fast | NOD initial | Mean Error | RMSE |
|------------------------|------------|------------|---------------|-------------|------------|------|
| | L/mmol-day | L/mmol-day | | mmol/g | | |
| Complete condition | 0.0317 | 5.66E-07 | 0.11 | 0.0212 | 0.020 | 0.73 |
| Once per day condition | 0.0151 | 1.00E-07 | 0.15 | 0.0208 | 0.011 | 0.73 |
| Static condition | 0.0072 | 2.56E-07 | 0.18 | 0.0157 | -0.026 | 0.53 |
| Total condition | 0.0128 | 1.00E-07 | 0.17 | 0.0165 | -0.010 | 0.72 |

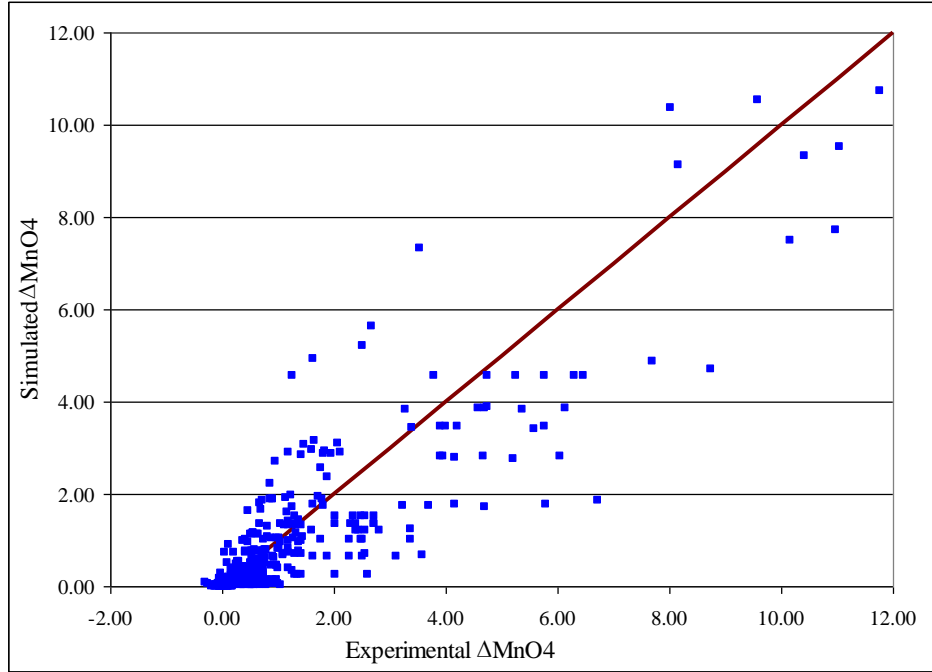


Figure 2-5 Comparison of Observed Values of ΔMnO_4 with Model 5 Simulation Results (all data for Soil C)

2.3.6 Model 6 – Second Order Loss of MnO_4 with Instantaneous and Slow NOD

Model 6 is similar to Model 5. However, the reaction between MnO_4 and fast NOD is assumed to occur so quickly, that it is essentially instantaneous. The instantaneous change in permanganate (M) and instantaneous NOD (N_I) are calculated by an if→then statement,

When concentration of $M > N_I * \rho_B / n$

$$M = M - \rho_B * N_I / n \text{ and } N_I = 0 \text{ otherwise } M = 0 \text{ and } N_I = N_I - M * n / \rho_B$$

Once the instantaneous reaction is complete, the change in permanganate (M) and slow NOD (N_S) are calculated by solving equations 2-6a and 2-6b.

$$\frac{dM}{dt} = -\rho_B k_{2S} N_S M / n \quad (2-6a)$$

$$\frac{dN_S}{dt} = -k_{2S} N_S M \quad (2-6b)$$

k_{2S} = 2nd order Slow NOD consumption rate (L mmol⁻¹ d⁻¹)

Experimental results are compared to simulated values for Model 6 in **Figure 2-6** and **Table 2-9**. Error statistics for Model 6 were very similar to Models 4 and 5 indicating that representing the reaction between ‘fast’ NOD and MnO₄ as an instantaneous reaction did not significantly hurt model performance. However, Model 6 run times were significantly shorter than Model 5. This would be a significant advantage when simulating complex 3-D aquifers.

Table 2-9 Statistical Result of Model 6 Evaluation

| Mixing Condition | k_{2S} | Fraction Instantaneous | NOD initial | Mean Error | RMSE |
|------------------------|------------|------------------------|-------------|------------|------|
| | L/mmol-day | | mmol/g | | |
| Complete condition | 0.0284 | 0.0239 | 0.0023 | -0.14 | 0.73 |
| Once per day condition | 0.0141 | 0.0200 | 0.0031 | -0.08 | 0.74 |
| Static condition | 0.0068 | 0.0109 | 0.0028 | -0.15 | 0.53 |
| Total condition | 0.0115 | 0.0200 | 0.0029 | -0.15 | 0.72 |

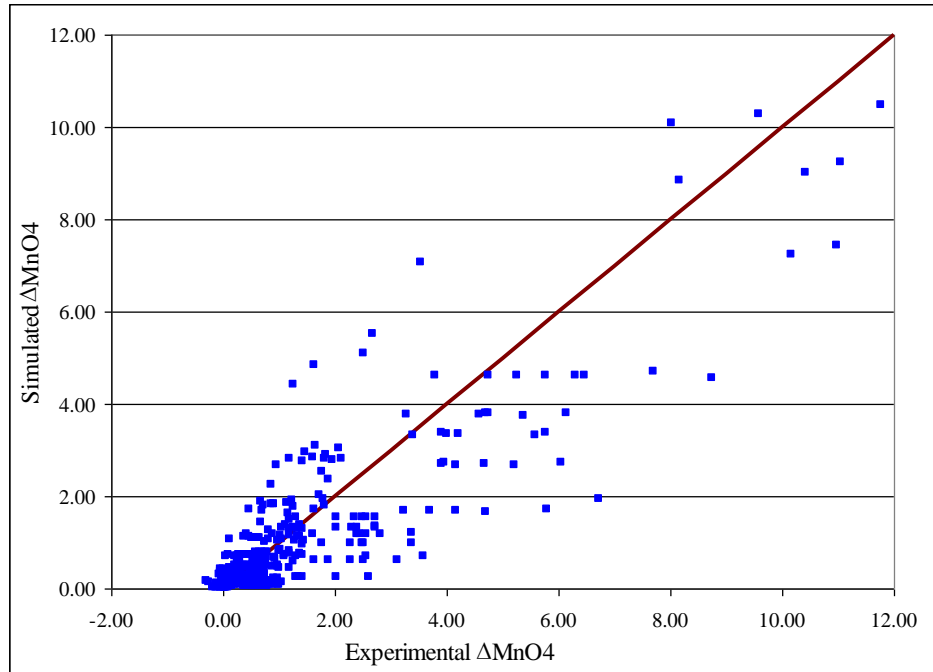


Figure 2-6 Comparison of Observed Values of ΔMnO_4 with Model 6 Simulation Results (all data for Soil C)

2.3.7 Kinetic Model Evaluation Summary

Six kinetic models were developed and calibrated to experimental measurements of NOD exerted by Soil C from MMR. The zero order and first order models (Models 1, 2 and 3) provided a relatively poor fit to the experimental results and will not be considered further.

All of the 2nd order models (4, 5 and 6) provided a relatively good fit to the experimental results. The RMSE was 0.72 for all 2nd order models using all of the Soil C data (total condition). The essentially identical performance of Models 4, 5 and 6 should not be surprising given the similar structure of each model.

Table 2-10 compares the estimated coefficients for Models 4, 5 and 6. In Model 5, the slow NOD reaction coefficient is so low (less than 10^{-6} L/mmol-d), that the slow NOD is essentially non-reactive over the 28 day incubation period. Consequently, the estimated values of total NOD in Model 4 are identical to fast NOD values in Model 5 and 2nd order rate coefficients in Model 4 are identical to the

fast 2nd order rate coefficients in Model 5. For practical purposes, the best fit parameter estimates for Models 4 and 5 are identical, and consequently the performance of these models is equivalent. Similarly, estimated values of total NOD for Models 4 and 6 are identical and performance of these models in matching the experimental data is equivalent. Estimated values for the 2nd order reaction rate in Model 6 are slightly lower than for Model 4 because of a small portion of the NOD in Model 6 (1-2%) reacts instantaneously. In summary, the overall performance and parameter estimates generated by Models 4, 5 and 6 are essentially identical for MMR Soil C.

Table 2-10 Best Fit Coefficients for Model 4, 5, and 6

| Model 4 | | Model 5 | | | Model 6 | | |
|--------------------|----------------------|------------------------|-----------------------|-----------------------|------------------|-------------------------|-----------------------|
| NOD initial | k₂ | NOD_F | k_{2F} | k_{2S} | Total NOD | Instant Fraction | k_{2S} |
| mmol/g | L/mmol-d | mmol/g | L/mmol-d | L/mmol-d | mmol/g | | L/mmol-d |
| 0.0023 | 0.032 | 0.0023 | 0.032 | 5.7E-07 | 0.0023 | 0.024 | 0.028 |
| 0.0031 | 0.015 | 0.0031 | 0.015 | 1.0E-07 | 0.0031 | 0.020 | 0.014 |
| 0.0028 | 0.007 | 0.0028 | 0.007 | 2.6E-07 | 0.0028 | 0.011 | 0.007 |
| 0.0029 | 0.013 | 0.0028 | 0.013 | 1.0E-07 | 0.0029 | 0.020 | 0.012 |

Given that Models 4, 5, and 6 all provide an equally good fit to the experimental data and provide similar parameter estimates, there is no specific reason to select one model over another. However, prior research by other investigators (Mumford et al. 2005, Mumford et al. 2004, and Xu 2006) indicates that soil NOD often contains fractions that react more rapidly and more slowly. Models 5 and 6 have the capability of simulating fast and slow fractions, while Model 4 does not. Model 5 did not provide a significantly improved fit compared to Model 6, but did take significantly longer to run due to the short computational time step required. Model 6 will be used in future modeling work. Model 6 performed as well as Model 4, and retains the capability of simulating fast and slow fractions, and did not require

significantly longer run times than Model 4. If the instantaneous fraction in Model 6 is set to zero, Models 4 and 6 are identical.

2.4 MMR Best Fit Parameter

In Chapter 4, a field scale groundwater flow, transport and reaction model will be used to simulate MnO_4 distribution and contaminant destruction in a large scale pilot test conducted at MMR. Estimates of the Model 6 kinetic parameters are required to calibrate this model.

Soil samples were collected from three depths (Samples A, B and C) in the vicinity of the MMR pilot test and tested by Dr. Michelle Crimi to provide NOD estimates. Characteristics of these soils are summarized in **Table 2-11**. Soil B was visually different than Soils A and C with less silt. Soil A is collected from the deepest location, C is middle and B is the shallowest location of injection well. The Unified Soil Classification System (USCS) define Soil A as SM and Soil B as SP which means silty sand and poor graded sand as well. Soil C is mix of undefined soil and SM.

Table 2-11 MMR Soil Sample Comparison

| Soil | A | B | C |
|------------------------------|---------------|---------------|-----------------------|
| Depth (ft) | 185' – 189' | 157' – 159.3' | 172' – 176.3' |
| USCS | SM | SP | SM + undefined |
| Texture | Silt and Sand | Sand | Silt and unknown soil |
| Hydro. Conductivity (ft/day) | 22 | 194 | 194 - 22 |

The experimental protocol followed for the three soils samples were similar, but not identical. Soil C was tested with all three mixing treatments (complete mixing, mix once per day, and static). Soil A was tested with static and once per day mixing. Soil B was tested with complete and once per day mixing. This resulted in a total of ten mixing-soil combinations resulting in ten sets of parameter estimates. Model 6 kinetic parameters were estimated for each soil-mixing combination

following the procedure previously described. Estimated values of total NOD, the slow NOD reaction rate, and fraction instantaneous NOD are shown in **Table 2-12** for each of the ten soil-mixing combinations.

Table 2-12a Best Fit Parameter Estimates for MMR Soils – Initial NOD (mmol/g)

| Mixing Condition | Soil A | Soil B | Soil C |
|------------------|--------|--------|--------|
| Static | 0.0032 | NA | 0.0028 |
| Once per day | 0.0028 | 0.0051 | 0.0031 |
| Complete | NA | 0.0077 | 0.0023 |
| All Data | 0.0027 | 0.0061 | 0.0029 |

Table 2-12b Best Fit Parameter Estimates for MMR Soils – Slow Reaction Rate (k_{2S}) (L/mmol-d)

| Mixing Condition | Soil A | Soil B | Soil C |
|------------------|--------|--------|--------|
| Static | 0.006 | NA | 0.007 |
| Once per day | 0.016 | 0.016 | 0.014 |
| Complete | NA | 0.017 | 0.028 |
| All Data | 0.013 | 0.025 | 0.012 |

Table 2-12c Best Fit Parameter Estimates for MMR Soils – Fraction Instantaneous

| Mixing Condition | Soil A | Soil B | Soil C |
|------------------|--------|--------|--------|
| Static | 0.085 | NA | 0.020 |
| Once per day | 0.093 | 0.096 | 0.020 |
| Complete | NA | 0.060 | 0.024 |
| All Data | 0.097 | 0.069 | 0.020 |

The total NOD of Soil B was significantly higher than for Soils A and C, which is consistent with the different visual appearance of this material. The instantaneous fraction was less than 10% for all the soils varying from 2.0% to 9.7% of the total NOD. The Slow Reaction Rate (k_{2S}) for all soils and mixing conditions

was relatively consistent varying from 0.007 to 0.025 L/mmol-d. An initial value of the effective 1st order decay coefficient (Ke) for permanganate can be estimated as

$$Ke = \rho_B k_{2S} N_S / n$$

Using this approach, the initial effective decay rate for permanganate varied from 0.1 to 1.0 per day with an average of 0.5 per day. This indicates the ‘slow’ NOD is reasonably reactive and could result in reasonably rapid depletion of permanganate.

In Chapter 3, a model is developed and applied to simulate the ISCO of TCE in a large scale field pilot test at MMR. Estimates of each of the Model 6 kinetic parameters will be required to calibrate this model to the MMR field site. The results presented above indicate that mixing condition has a modest impact of the different kinetic parameters. As a consequence, all the data for the different mixing conditions was grouped together and analyzed as a single data set. **Table 2-13** shows the best estimates of the Model 6 parameters for three groups of data: (1) Soil A and C combined, (2) Soil B and (3) Soil A, B and C combined. Soils A and B were grouped together based on their similar NOD characteristics and visual appearance.

Table 2-13 Parameter Set for MMR

| Soil Type | Fraction Instantaneous | Initial NOD | Slow Reaction Rate | N* | RMSE |
|------------------|-----------------------------------|------------------------|---------------------------|-----------|-------------|
| | | mmol/g | L/mmol-d | | |
| A,C | 0.09 | 0.0026 | 0.0125 | 57 | 1.17 |
| B | 0.07 | 0.0061 | 0.025 | 12 | 1.07 |
| A,B,C | 0.087 | 0.0038 | 0.0166 | 69 | 0.77 |

* N is the number of individual incubations used to generate these estimates. Each incubation typically had 16 separate permanganate measurements.

CHAPTER 3 MODEL CALIBRATION AGAINST FIELD DATA FROM MMR PILOT TEST

3.1 Introduction

A pilot test of in situ chemical oxidation (ISCO) using permanganate was conducted at the Massachusetts Military Reservation in Fall 2007 to evaluate the potential applicability of ISCO for treatment of the CS-10 contaminant plume. Results from this pilot test will be used to evaluate the capability of a groundwater flow, transport and reaction model to simulate ISCO in the subsurface. This model has been developed using the previously described Model 6 and NOD kinetic parameters estimated in Chapter 2. Three different parameter sets (**Table 2-13**) which were generated from laboratory NOD measurements and are used in the model calibration.

3.2 Massachusetts Military Reservation (MMR)

Massachusetts Military Reservation (MMR) is located on the south-western portion of Cape Cod, Massachusetts near the towns of Bourne, Mashpee, Sandwich, and Falmouth (**Figure 3-1**).

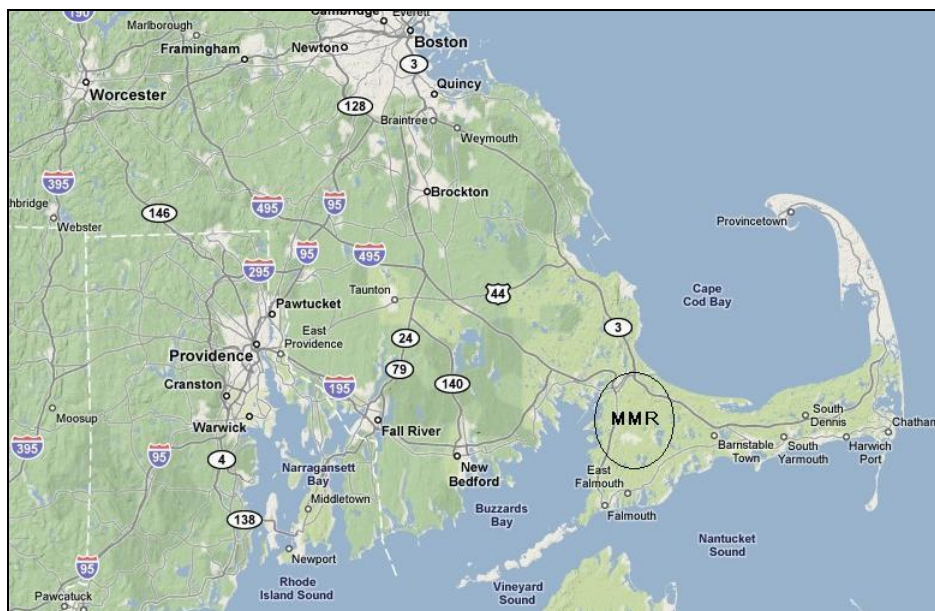


Figure 3-1 Location of MMR on Cape Cod, Massachusetts

The MMR have been used for military purposes since 1911. Although the occupants and boundary have been changed since MMR was established in the 1930s, the facility has always provided training and housing space for Air Force and/or Army units. Work at MMR includes training and maneuvers, military aircraft/vehicle operations, maintenance (repair, cleaning, oil change and body work), and support. The hazardous wastes generated at the site were commonly disposed in landfills, drywells, sumps, and occasionally burned at firefighter-training areas. This has resulted in multiple contaminant plumes. The contaminants detected in groundwater at MMR include carbon tetrachloride (CCl_4), trichloroethene (TCE), perchloroethene (PCE), ethylene dibromide (EDB), and benzene. Hydrologic condition at MMR result in high groundwater flow velocities (1-2 feet per day) and a radial flow pattern where the plumes migrate outward from the center of the site towards water bodies on the site boundaries (**Figure 3-2**) (AFCEE 2007a).

Chemical Spill 10 (CS-10) located in the southern portion of MMR is the focus of this study. Contaminants of concern in the CS-10 plume are TCE and PCE with maximum observed concentrations of 602 and 119 $\mu\text{g/L}$, respectively. These

This map illustrates the Massachusetts Military Reservation and its surrounding areas, including Towns of Bourne, Sandwich, Falmouth, and Mashpee. It highlights several groundwater plumes (CS-19, CS-10, CS-23, CS-21, CS-20, CS-4, FS-12, FS-1, FS-28, FS-29) and their respective treatment facilities (LF-1, CS-10, FS-12, Sandwich Road, FS-1, Ashumet Valley, FS-28). A note indicates that there are other groundwater plumes in the area not part of the IRP and therefore not depicted on the map. For further information, please call Kristina Curley at (508) 968-5526.

26

3.3 Pilot Test

The ISCO pilot test was conducted near monitor well 03MW1024 because of the relatively high TCE concentrations in this area and the opportunity to reduce future remediation costs. The geology of this site is similar to other portions of the CS-10 plume and other areas at MMR, potentially allowing results from this site to be extrapolated to other locations. The test area is also easily accessible for power supplies, equipment, personnel and is a secure location (CH2MHILL 2007).

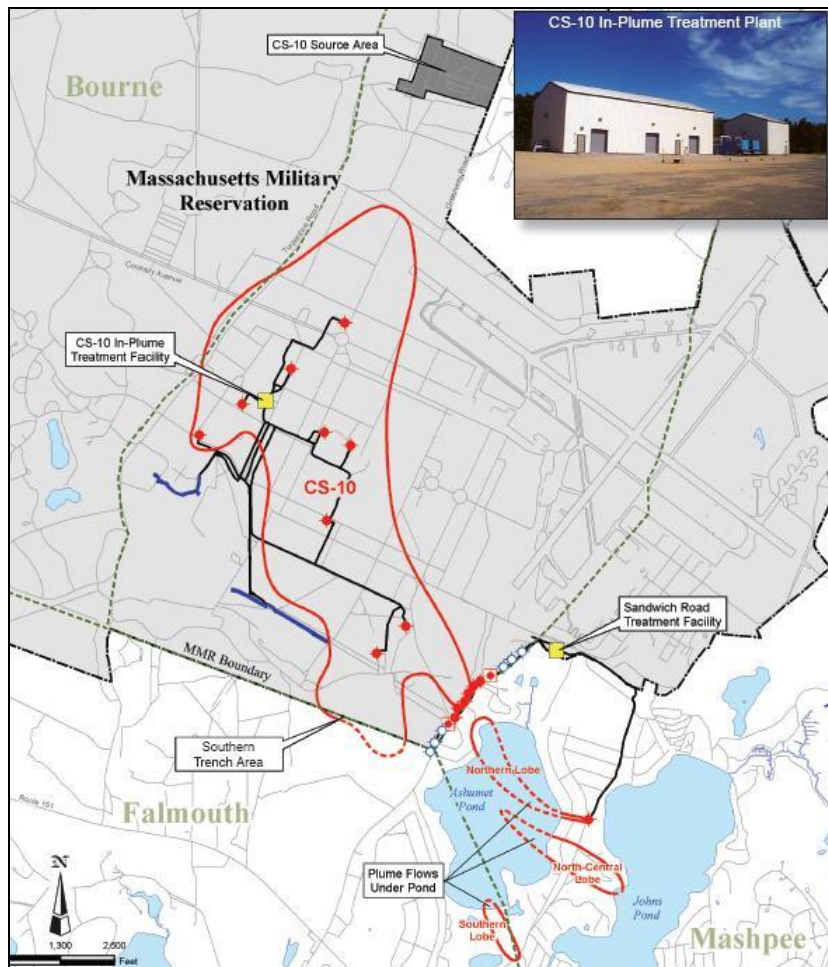


Figure 3-3 Map of CS-10 Plume (grey area represent MMR, red line represent plume boundary, AFCEE 2007b)

TCE contamination at the pilot test site is distributed in two major zones, a shallow zone extending from 150 to 205 feet below ground surface (ft bgs) with concentration range from TCE varying from 18 to 590 µg/L, and a deep zone extending from 230 to 295 ft bgs with TCE varying from 12 to 98 µg/L. The most of the soil in pilot test area is sand. However, a fine sand /silty sand unit is located between 175 and 201 ft bgs, at approximately the same depth as the zone of maximum contaminant concentration (CH2MHILL 2007).

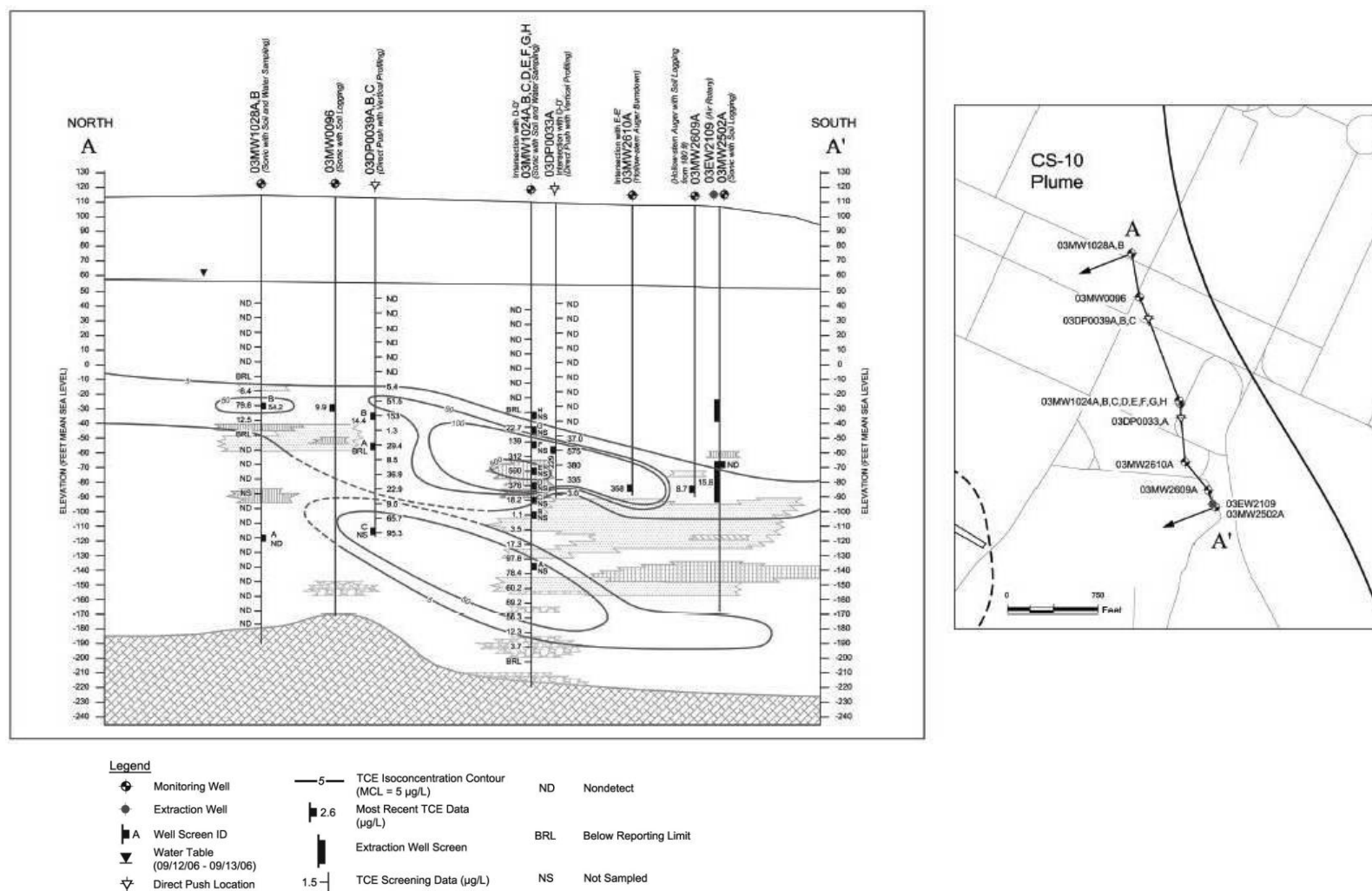


Figure 3-4 Map of Cross Section of Pilot Test Area (CH2MHILL 2007)

The pilot test area contains a single injection well and seven monitoring wells. The injection well (03IJW001) has three separate screened intervals allowing injection at different depths. The monitoring wells are installed up-gradient, cross-gradient, and down-gradient of the injection location with 22 well screens allowing monitoring at different depths. **Table 3-1** provides details on the screened interval of each injection and monitoring well.

The pilot test design consisted of injecting 5,000 mg/L sodium permanganate (NaMnO_4) for 10 hours per day for four days. This solution was to be injected into three injection wells simultaneously at 10 gallons per minute (gpm) for a total flow of 30 gpm. The plan was to inject a total volume of 72,000 gallons of water containing 1363 Kg NaMnO_4 . The actual injection flow rates and concentrations varied somewhat from this plan due to problems in maintaining a constant dilution rate and difficulty in maintaining high injection rates in the lower permeability zones.

TCE and permanganate concentrations in the injection and selected monitor wells were measured five times between November 2007 and May 2008. Monitoring results are presented in **Table 3-2** and **3-3**. TCE was not monitored when the groundwater had a purple color indicating the presence of dissolved permanganate. Permanganate concentrations were determined by measuring manganese concentration in the water with a Hach Test Kit.

Table 3-1 Wells of Pilot Test

| Well Cluster | Purpose (target of monitoring) | General Location (from injection well) | Top of Screen (ft bgs) | Bottom of Screen (ft bgs) |
|---------------------|---|---|-----------------------------------|--------------------------------------|
| 03IJW001A | Oxidant injection | - | 185.3 | 190.3 |
| 03IJW001B | | | 172.2 | 177.2 |
| 03IJW001C | | | 157.15 | 162.15 |
| 03MW1024A | Vertical migration of the injected oxidant | 25 ft Down-gradient | 245.29 | 250 |
| 03MW1024B | | | 210.47 | 215 |
| 03MW1024C | | | 200.29 | 205 |
| 03MW1024D | | | 190.29 | 195 |
| 03MW1024E | | | 180.02 | 185 |
| 03MW1024F | | | 162.02 | 167 |
| 03MW1024G | | | 152.24 | 157 |
| 03MW1024H | | | 142.24 | 147 |
| 03MW1032A | TCE concentrations approaching the test area | 30 ft Up-gradient | 185.37 | 190.37 |
| 03MW1032B | | | 172.63 | 177.63 |
| 03MW1032C | | | 157.46 | 162.46 |
| 03MW1033A | Tracking the changes in oxidant and TCE along the centerline of the flow | 60 ft Down-gradient | 200.1 | 205.1 |
| 03MW1033B | | | 172.28 | 177.28 |
| 03MW1033C | | | 147.32 | 152.32 |
| 03MW1034A | Horizontal migration of the injected permanganate | 35 ft SE Down-gradient | 200.38 | 205.38 |
| 03MW1034B | | | 173.37 | 178.37 |
| 03MW1034C | | | 147.08 | 152.08 |
| 03MW1035A | | 35 ft SW Down-gradient | 200.02 | 205.02 |
| 03MW1035B | | | 172.41 | 177.41 |
| 03MW1035C | | | 152.04 | 157.04 |
| 03MW1036A | | 65 ft SE Down-gradient | | |
| 03MW1037A | | 65 ft SW Down-gradient | | |

Table 3-2 TCE Monitoring Results

| Well Identifier | TCE (µg/L) | | | | |
|-----------------|------------|------------|-----------|-----------|-----------|
| | Baseline | 12/12/2007 | 2/19/2008 | 3/19/2008 | 5/19/2008 |
| 03DP0033A | 175 | NS | purple | 212 | purple |
| 03IJW001A | 204 | NS | purple | purple | purple |
| 03IJW001B | 70.3 | NS | NA | NA | NA |
| 03IJW001C | 84.4 | NS | NA | NA | NA |
| 03MW1024A | 92.4 | NS | NS | NS | NS |
| 03MW1024B | BRL | BRL | 1.4 | 1.7 | 1.7 |
| 03MW1024C | 112 | 253 | 302 | purple | purple |
| 03MW1024D | 450 | 352 | purple | purple | purple |
| 03MW1024E | 206 | purple | purple | purple | purple |
| 03MW1024F | 184 | purple | purple | purple | 157 |
| 03MW1024G | 7.5 | purple | 6.8 | 6.2 | 5.3 |
| 03MW1024H | 1.6 | BRL | 0.18 | ND | BRL |
| 03MW1032A | 402 | 459 | 260 | 447 | 527 |
| 03MW1032B | 94.6 | 41.2 | 47.5 | 46.1 | 36.6 |
| 03MW1032C | 6.6 | 5.9 | 4.3 | 4.5 | 3.4 |
| 03MW1033A | 8.2 | 9 | 4.4 | 9.4 | 12.8 |
| 03MW1033B | 197 | 150 | purple | purple | purple |
| 03MW1033C | 1.3 | BRL | BRL | BRL | ND |
| 03MW1034A | ND | ND | 1 | ND | ND |
| 03MW1034B | 71.9 | purple | purple | purple | purple |
| 03MW1034C | BRL | BRL | 0.3 | BRL | 2.6 |
| 03MW1035A | 66.9 | 42.6 | 80.2 | 94.3 | 121 |
| 03MW1035B | 118 | 151 | 150 | 157 | 195 |
| 03MW1035C | 4.5 | 6.6 | 6.9 | 5.8 | |
| 03MW1036A | 148 | 151 | purple | purple | purple |
| 03MW1037A | 229 | 243 | 248 | 219 | 215 |

*Purple samples were not analyzed for TCE.

Table 3-3 Permanganate Monitoring Results

| Well Identifier | Permanganate (mg/L) | | | | | | | | |
|-----------------|---------------------|---------------|---------------|---------------|---------------|--------------|--------------|-------------|--------------|
| | 11/14 2007 | 11/16 2007 | 11/20 2007 | 11/28 2007 | Dec. 2007* | Jan. 2008 | Feb. 2008 | Mar. 008 | May. 2008 |
| 03DP0033A | NS | NS | NS | NS | NS | 258.3 | 5.2 | 0.0 | 100.2 |
| 03IJW001A | NS | NS | NS | NS | 3125.4 | 6005.5 | 8007.3 | 7361.6 | 4236.1 |
| 03IJW001B | NS | NS | NS | NS | 55.3 | 0.8 | 0.3 | 1.0 | 0.5 |
| 03IJW001C | NS | NS | NS | NS | 173.1 | 87.8 | 2.8 | 0.0 | 0.5 |
| 03MW1024B | 0.3 | 0.0 | 0.3 | 0.0 | 0.0 | 0.0 | 0.3 | 0.0 | 0.0 |
| 03MW1024C | 15.0 | 0.0 | 0.8 | 0.8 | 0.0 | 0.8 | 0.0 | 67.2 | 50.9 |
| 03MW1024D | 0.0 | 0.0 | 0.0 | 0.0 | 0.0 | 93.0 | 103.3 | 250.6 | 671.6 |
| 03MW1024E | 0.0 | 0.0 | 0.0 | 0.0 | 124.0 | 3616.2 | 4003.7 | 2763.8 | 904.1 |
| 03MW1024F | 4.4 | 258.3 | 1472.3 | 1730.6 | 1033.2 | 155.0 | 72.3 | 43.9 | 0.3 |
| 03MW1024G | 0.5 | 0.0 | 0.0 | 2660.5 | 981.5 | 0.3 | 0.0 | 1.5 | 0.0 |
| 03MW1024H | 0.0 | 0.0 | 0.3 | 0.0 | 0.3 | 0.0 | 0.0 | 0.0 | 0.0 |
| 03MW1032A | 3.4 | 0.3 | 0.3 | 0.0 | 0.0 | 0.8 | 0.5 | 0.0 | 0.0 |
| 03MW1032B | 19.1 | 0.0 | 0.3 | 2.8 | 0.0 | 0.0 | 0.0 | 0.0 | 0.3 |
| 03MW1032C | 7.7 | 0.3 | 0.0 | 0.5 | 0.3 | 0.0 | 4.4 | 10.6 | 0.0 |
| 03MW1033A | 7.5 | 0.0 | 0.5 | 0.3 | 0.3 | 0.0 | 0.0 | 0.3 | 0.0 |
| 03MW1033B | 2.6 | 0.0 | 0.0 | 0.0 | 0.0 | 0.0 | 1743.5 | 2456.9 | 50.6 |
| 03MW1033C | 1.3 | 0.0 | 0.0 | 0.3 | 0.0 | 0.0 | 0.0 | 0.0 | 0.0 |
| 03MW1034A | 15.2 | 2.1 | 1.8 | 0.5 | 0.5 | 28.4 | 0.8 | 5.7 | 0.3 |
| 03MW1034B | 4.6 | 0.0 | 0.0 | 0.0 | 1291.5 | 5553.5 | 3809.9 | 1485.2 | 15.2 |
| 03MW1034C | 2.1 | 0.0 | 0.0 | 0.0 | 0.0 | 0.0 | 0.0 | 0.0 | 0.0 |
| 03MW1035A | 15.0 | 1.0 | 0.0 | 0.5 | 0.0 | 0.5 | 0.3 | 0.0 | 0.0 |
| 03MW1035B | 3.9 | 0.0 | 0.3 | 0.0 | 0.3 | 0.3 | 0.0 | 0.0 | 0.0 |
| 03MW1035C | 0.5 | 0.3 | 0.0 | 0.0 | 0.0 | 0.3 | 0.3 | 0.0 | 0.3 |
| 03MW1036A | 3.6 | 0.0 | 0.3 | 0.5 | 0.3 | 0.3 | 20.4 | 69.7 | 594.1 |
| 03MW1037A | 0.0 | 0.0 | 0.5 | 0.3 | 0.0 | 0.0 | 0.0 | 0.0 | 0.3 |

Key: BRL = below reporting limit

NA = not analyzed

ND = not detected

NS = not sampled

3.4 Modeling of MMR Pilot Test

3.4.1 Reaction Kinetics

The transport and consumption of permanganate (M) and the target groundwater contaminant (C) was simulated using the standard forms of the advection-dispersion equations 3-1.

$$\frac{\partial M}{\partial t} = \frac{\partial}{\partial x} \left(D \frac{\partial M}{\partial x} \right) - \frac{\partial}{\partial x} (vM) - \Gamma_M \quad (3-1a)$$

$$R_C \frac{\partial C}{\partial t} = \frac{\partial}{\partial x} \left(D \frac{\partial C}{\partial x} \right) - \frac{\partial}{\partial x} (vC) - \Gamma_C \quad (3-1b)$$

where,

| | |
|------------------|--|
| M = | MnO ₄ concentration (mol L ⁻¹) |
| C = | Contaminant concentration (mol L ⁻¹) |
| t = | Time |
| x = | Distance |
| D = | Dispersion coefficient (L ² T ⁻¹) |
| v = | Pore water velocity (LT ⁻¹) |
| R _C = | linear equilibrium retardation factor of the contaminant |
| Γ = | Chemical reaction terms |

Kinetics expressions to describe the loss of permanganate (M) by NOD are based on Model 6 from Chapter 2. The reaction between permanganate and the contaminant is assumed to be instantaneous based published reaction rates which indicate that reactions between permanganate and PCE or TCE are very rapid. Overall, the loss of M and C are described by the following three step sequence.

(1) An instantaneous reaction between M and the contaminant (C) where

When concentration of $M > CR_C Y_{M/C}$

$$M = M - CR_C Y_{M/C} \text{ and } C = 0 \text{ otherwise } M = 0 \text{ and } C = C - M / RY_{M/C}$$

(2) An instantaneous reaction between M and the instantaneous NOD (N_I) where,

When concentration of $M > N_I * \rho_B / n$

$$M = M - \rho_B * N_I / n \text{ and } N_I = 0 \text{ otherwise } M = 0 \text{ and } N_I = N_I - M * n / \rho_B$$

(3) A second order reaction between M and slow NOD (N_S) where

$$\frac{dM}{dt} = -\rho_B k_{2S} N_S M / n \quad (3-2a)$$

$$\frac{dN_S}{dt} = -k_{2S} N_S M \quad (3-2b)$$

and,

N_I = Instantaneous NOD (mol Kg^{-1})

N_S = Slow NOD (mol Kg^{-1})

ρ_B = bulk density (Kg L^{-1})

$Y_{M/C}$ = molar ratio of M to C consumed (mol/mol)

k_{2S} = 2nd order Slow NOD consumption rate ($\text{L mol}^{-1} \text{d}^{-1}$)

3.4.2 Numerical Implementation

Groundwater flow and solute transport were simulated using the MODFLOW (Harbaugh et al., 2000) and RT3D (Clement 1997) engines within GMS (Aquaveo 2008). The chemical reactions between M, C, N_I and N_S were implemented through a FORTRAN 90 code compiled using Visual FORTRAN compiler in dynamic link

libraries (rxns.dll) and formatted to fit the user-defined reaction package in RT3D. Appendix A shows a comparison between the RT3D implementation of these equations and a 1-D analytical solution with a constant 1st order decay rate.

3.4.3 Model Setup

3.4.3.1 Grid and Initial Contaminant

The simulation grid for the pilot test consists of 560,560 cells with 98 columns by 143 rows by 40 layers. The cell size is non-uniform varying from 5 to 70 ft with smaller cells near the injection wells. Plan and profiles views of the model grid are presented in **Figure 3-5** and **3-6**.

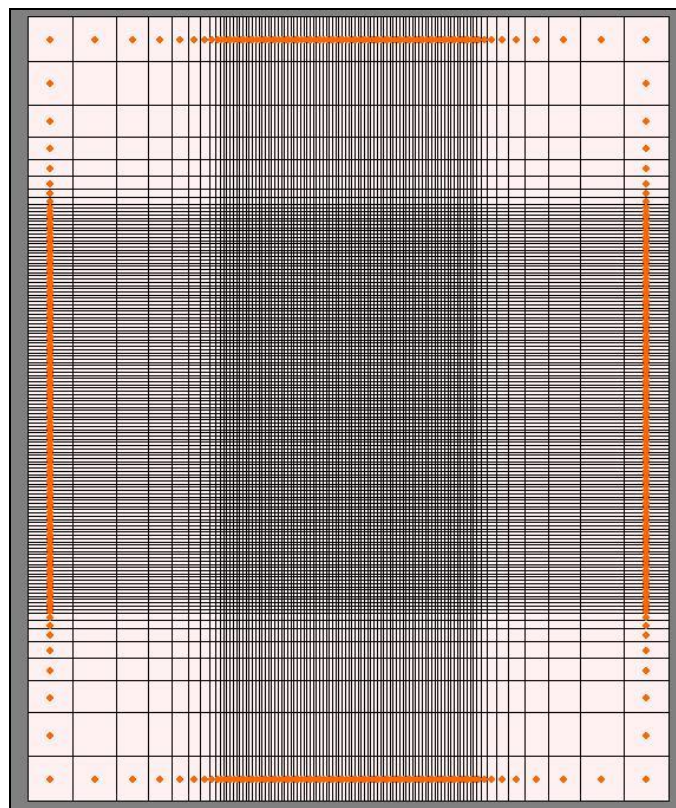


Figure 3-5 Plan View of MMR Pilot Test Simulation Grid

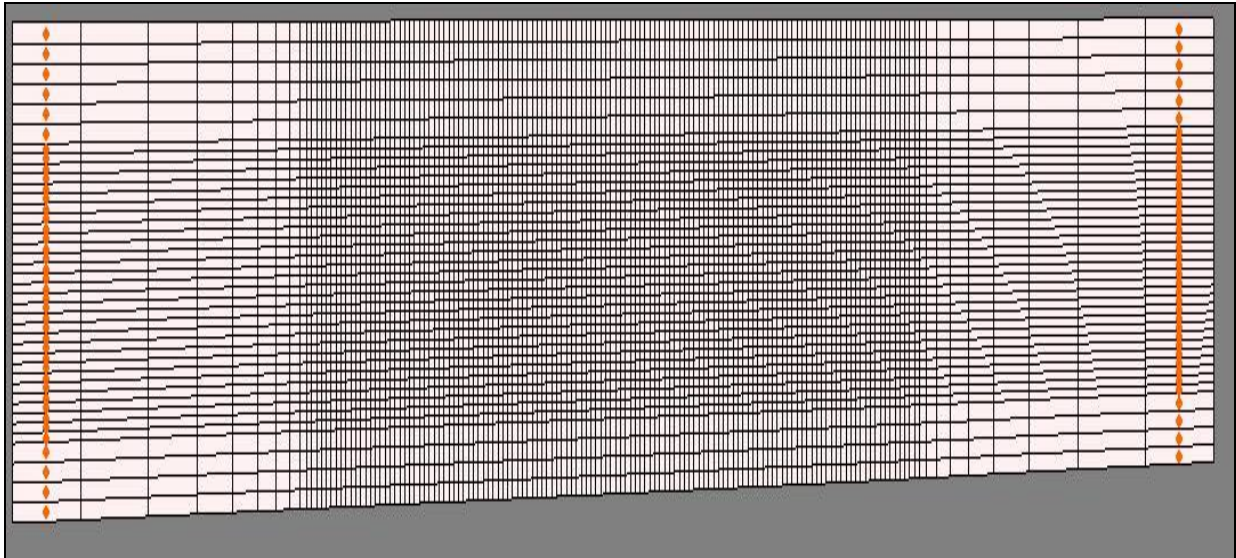


Figure 3-6 Profile View of MMR Pilot Test Simulation Grid

Figure 3-7 show the permeability distribution used in the numerical simulations. This permeability distribution was generated by Mr. John Glass of CH2MHILL based on multiple lithologic logs of the MMR site and the observed pressure response in injection and monitor wells during the pilot test. The higher permeability zones are represented by dark reds and lower permeability, silt layers by white and light pink.

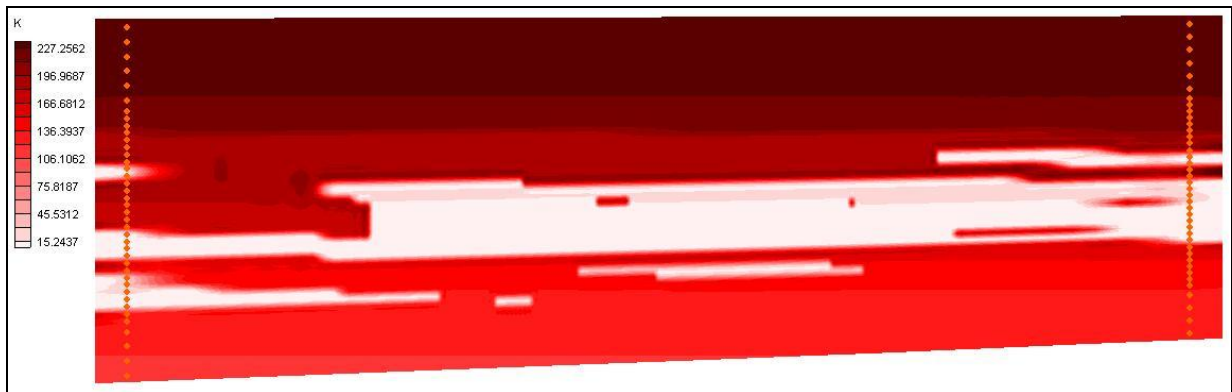


Figure 3-7 Cross-Section View of Permeability Distribution (deep red color indicates high permeability and white color indicates low permeability area)

The initial contaminant distribution in the aquifer was generated by spatial interpolation of measured TCE concentrations in monitor wells immediately prior to the start of the pilot test. For the MMR pilot test, monitoring data was available from 26 wells located in the center area with three observations below the method detection limit (MDL). The initial contaminant distribution was generated using the ‘Inverse Distance Weighted’ available within GMS. **Figure 3-8** show a plan view of the interpolated distribution. The monitor wells are generally aligned from north-west to south-east along the direction of groundwater flow.

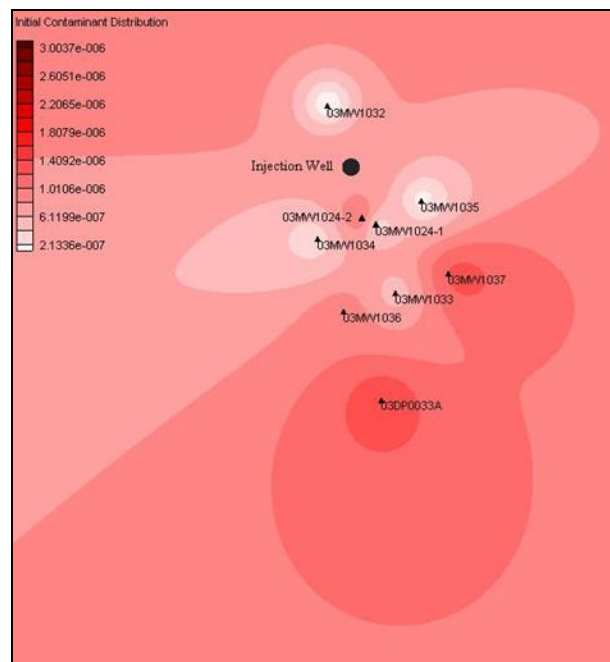


Figure 3-8 Plan View of 15th Layer of Model with Contaminants Distribution and Injection and Monitoring Wells

Figure 3-9 show the front view of model with injection well and monitoring wells. The black bar in the middle of figure is the injection well and blue boxes represent well screen locations. Thin lines indicate the monitoring well cluster locations with screen depth indicated by the black triangles.

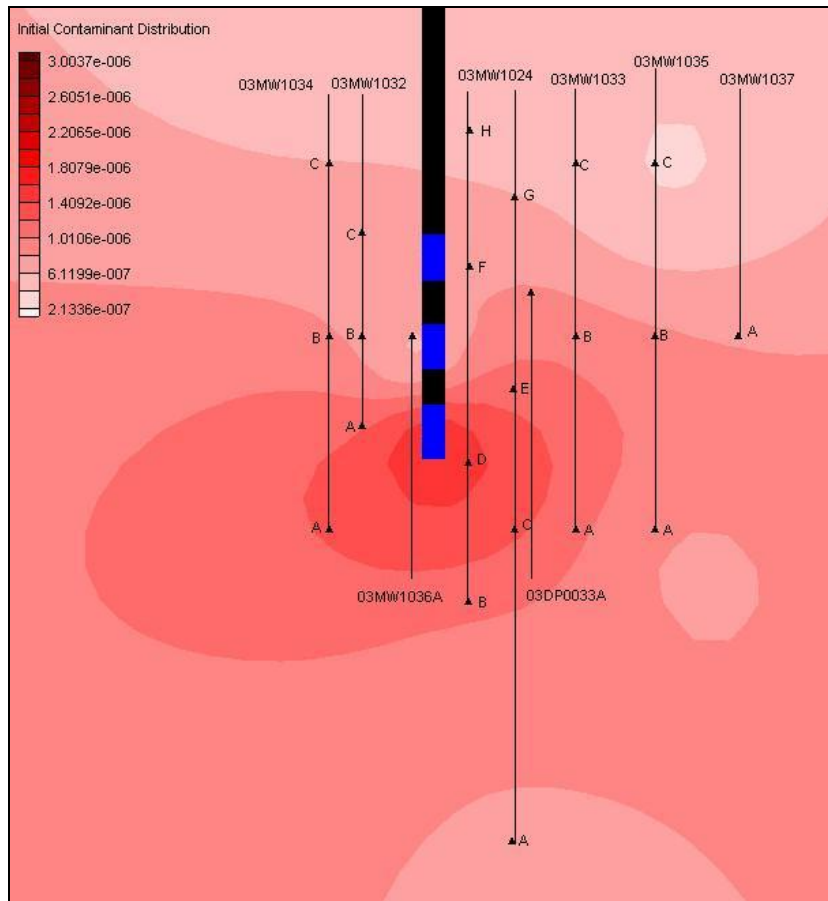


Figure 3-9 Front View of 50th Row of Model with Contaminants Distribution and Injection and Monitoring Wells (thick bar indicate injection well, blue box indicate well screen and triangle indicate monitoring well)

3.4.3.2 Oxidant Injection

Table 3-4 shows the injection rates and permanganate concentrations used in the model calibration. These flow rates and concentrations are based on monitoring data collected by CH2MHILL during the pilot test. Approximately 6% more water was injected and the injection period extended over five days instead of the originally planned four day injection.

Table 3-4 Injection Flow Rates and Concentrations Used in Model Simulations

| | Dur. | Flow Rate | MnO₄ Conc. | Flow Rate | MnO₄ Conc. | Flow Rate | MnO₄ Conc. | Water Vol. | MnO₄ Mass |
|---------------------|-------------|--------------------|------------------------------|--------------------|------------------------------|--------------------|------------------------------|-------------------|-----------------------------|
| | day | ft ³ /d | mol/L | ft ³ /d | mol/L | ft ³ /d | mol/L | L | mol |
| 1 st day | 0.37 | 1,491 | 0.0498 | 1,592 | 0.0500 | 1,710 | 0.0491 | 50,804 | 2,523 |
| 2 nd day | 0.40 | 1,698 | 0.0000 | 1,353 | 0.0887 | 1,763 | 0.0425 | 55,009 | 2,227 |
| 3 rd day | 0.41 | 1,430 | 0.0000 | 1,913 | 0.0605 | 3,145 | 0.0277 | 74,646 | 2,333 |
| 4 th day | 0.40 | 1,572 | 0.0075 | 1,704 | 0.0059 | 2,907 | 0.0487 | 69,172 | 1,828 |
| 5 th day | 0.25 | 1,214 | 0.0000 | 1,777 | 0.0000 | 2,680 | 0.0000 | 40,595 | 0 |
| Total | | | | | | | | 290,225 | 8,911 |

* Dur. indicate duration

3.4.3.3 Reaction Parameters

Reaction parameters used in the model calibration were estimated from literature values and are presented in **Table 3-5**.

Table 3-5 List of Common Parameters Used in Calibration Model

| | | |
|---|----------|----------------------|
| TCE Retardation Factor | 10 | - |
| Molar ratio of MnO₄ to TCE consumed | 2 | - |
| Porosity | 0.25 | - |
| Bulk Density | 2 | kg/L |
| Longitudinal Dispersivity | 3.28 | ft |
| Horizontal Dispersivity | 0.328 | ft |
| Vertical Dispersivity | 0.0328 | ft |
| Molecular diffusion coefficient | 1.61E-13 | ft ² /day |

In Chapter 2, NOD kinetic parameters were estimated for three soils samples from MMR based on a total of ten soil-mixing combinations. Overall, the kinetic parameters were similar for all the tests indicating a low total NOD, less than 10% instantaneous NOD, and moderate slow reaction rate. However, the higher permeability soil B did have a significantly higher total NOD (0.0061 mmol/g) than soils A and C (0.0027 to 0.0029 mmol/g). It is not clear from the batch test results whether the difference in total NOD between soils B and A/C is significant.

A series of simulations were conducted to examine the sensitivity of the model simulation results to the NOD kinetic parameters and to determine if one parameter set provided a better fit to the monitoring data. Four different scenarios were evaluated. Scenarios 1, 2, and 3 use single values of the model parameters for the entire model domain. Scenario 1 uses parameter values from Soils A and C; scenario 2 uses parameter values for Soil B, and scenario 3 uses the average of values for Soils A, B, and C. Scenarios 4 use different values for high and low permeability zones in the model. High permeability zones are represented by Soil B and low permeability zones by Soils A and C. In the current implementation of the model, the slow reaction rate must be spatially uniform. Scenario 4 uses the averaged slow reaction rate for Soils A, B, and C. **Table 3-6** presents the values of each parameter used in the simulations

Table 3-6 The Details of 4 Different Scenarios

| Scenario | Soil Type | Fraction Instantaneous | Instantaneous NOD | Slow NOD | Slow Reaction Rate |
|----------|-----------|------------------------|-------------------|----------|--------------------|
| | | | mmol/g | mmol/g | L/mmol-d |
| 1 | A,C | 0.09 | 0.000234 | 0.002366 | 0.0125 |
| 2 | B | 0.07 | 0.000427 | 0.005673 | 0.025 |
| 3 | A,B,C | 0.087 | 0.000333 | 0.003466 | 0.0166 |
| 4 | B | 0.07 | 0.000427 | 0.005673 | 0.01875 |
| | A,C | 0.09 | 0.000234 | 0.002366 | |

3.5 Model Calibration

The pilot test was simulating using five different sets of NOD kinetic parameter (see **Table 3-6**). The goodness of fit was evaluated by comparing the simulated and observed permanganate and TCE distributions at various time points. Two different error statistics were used: (1) root mean squared error; and (2) a qualitative statistic indicating the presence or absence of a compound at each monitoring point.

3.5.1 Simple Scoring Error Statistics (SSES)

Permanganate reacts very rapidly with TCE. As a consequence, if permanganate reaches a zone, TCE will be rapidly reduced to zero. Under these conditions, the presence or absence of permanganate in a monitoring well is often a more important indicator of treatment, than the absolute concentration of permanganate or TCE concentration observed in that well.

To provide a more accurate representation of this condition, the simple scoring error statistic (SSES) was developed. Using the SSES procedure, a monitor well is considered ‘contacted’ if the concentration of a solute (MnO_4 or TCE) is greater than 1% of the maximum concentration observed at the site. Each monitor well is then evaluated to determine if the model accurately matched the field observations. For example, if both the field and monitoring data indicate that MnO_4 is present in one well during a single sampling event, that is counted as ‘matched’. Conversely, if the model indicates TCE is present (at over 1% of max. conc.) and the field data indicate TCE is below detection that observation is a ‘not matched’. The fractions of matched observations are then reported for both TCE and MnO_4 .

3.5.2 Model Calibration Results

Table 3-7a and **3-7b** show the Root Mean Square Error (RMSE), Observations Not Matched, Observations Matched, and Percent Matched for the

contaminant (TCE) and MnO₄. In general, all the scenarios provided a reasonably good match to the field observations. Scenario 4 appears to provide a slightly better fit to the data with a lower RMSE for TCE and higher SSES for TCE and MnO₄. The RMSE for MnO₄ generated by scenario 4 was slightly higher than for scenario 2. However, this difference is probably not significant given uncertainty in measured MnO₄ concentrations. In summary, each scenario provides an acceptable match to the field data, with a slightly better fit provided by scenario 4.

Table 3-7a Error Statistics between Simulated and Observed Contaminant (TCE)

| | Contaminant (TCE) | | | |
|-----------------|--------------------------|--------------------|----------------|------------------|
| Scenario | RMSE | Not Matched | Matched | % Matched |
| 1 | 5.8E-07 | 24 | 44 | 65% |
| 2 | 5.5E-07 | 23 | 45 | 66% |
| 3 | 5.6E-07 | 24 | 44 | 65% |
| 4 | 4.5E-07 | 20 | 48 | 71% |
| Best Result | 4 | 4 | 4 | 4 |

Table 3-7b Error Statistics between Simulated and Observed Permanganate

| | MnO₄ | | | |
|-----------------|------------------------|--------------------|----------------|------------------|
| Scenario | RMSE | Not Matched | Matched | % Matched |
| 1 | 3.2E-03 | 21 | 82 | 80% |
| 2 | 3.0E-03 | 24 | 79 | 77% |
| 3 | 3.1E-03 | 22 | 81 | 79% |
| 4 | 3.3E-03 | 18 | 85 | 83% |
| Best Result | 2 | 4 | 4 | 4 |

Figure 3-10a and **3-10b** show the simulated contaminant and permanganate distributions in a cross-section through the pilot test area at 6, 18, 30 and 90 days after the start of permanganate injection. Ground water flow is approximately right to left across the figure. The contaminant (TCE) is depleted (indicated by white) in the center of the pilot test area (**Figure 3-10a**) as permanganate migrates down-gradient (**Figure 3-10b**).

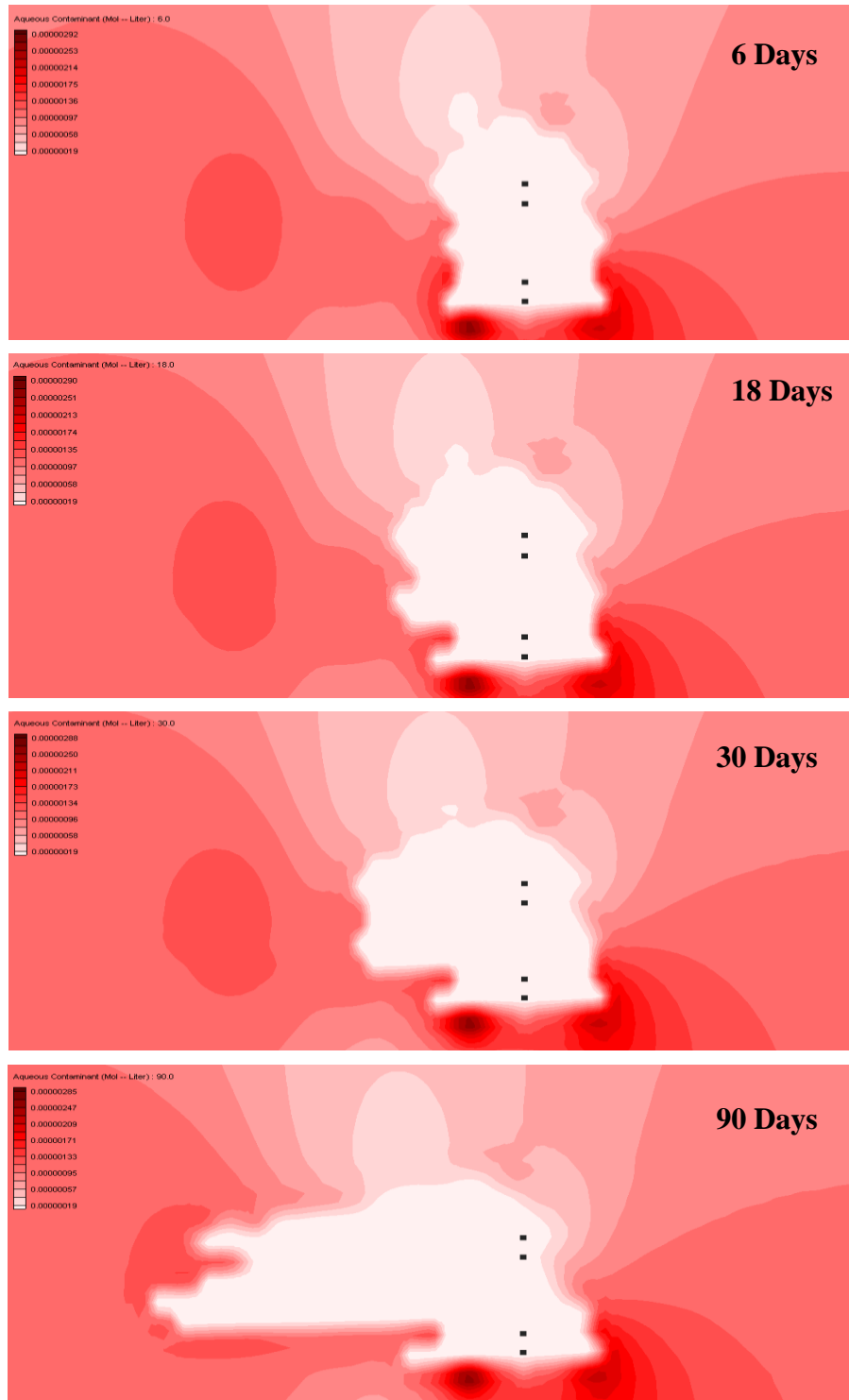


Figure 3-10a Profile View of Contaminant Distribution at 6, 18, 30 and 90 Days of Simulation with Scenario 4 (deep red indicate high concentration of contaminant)

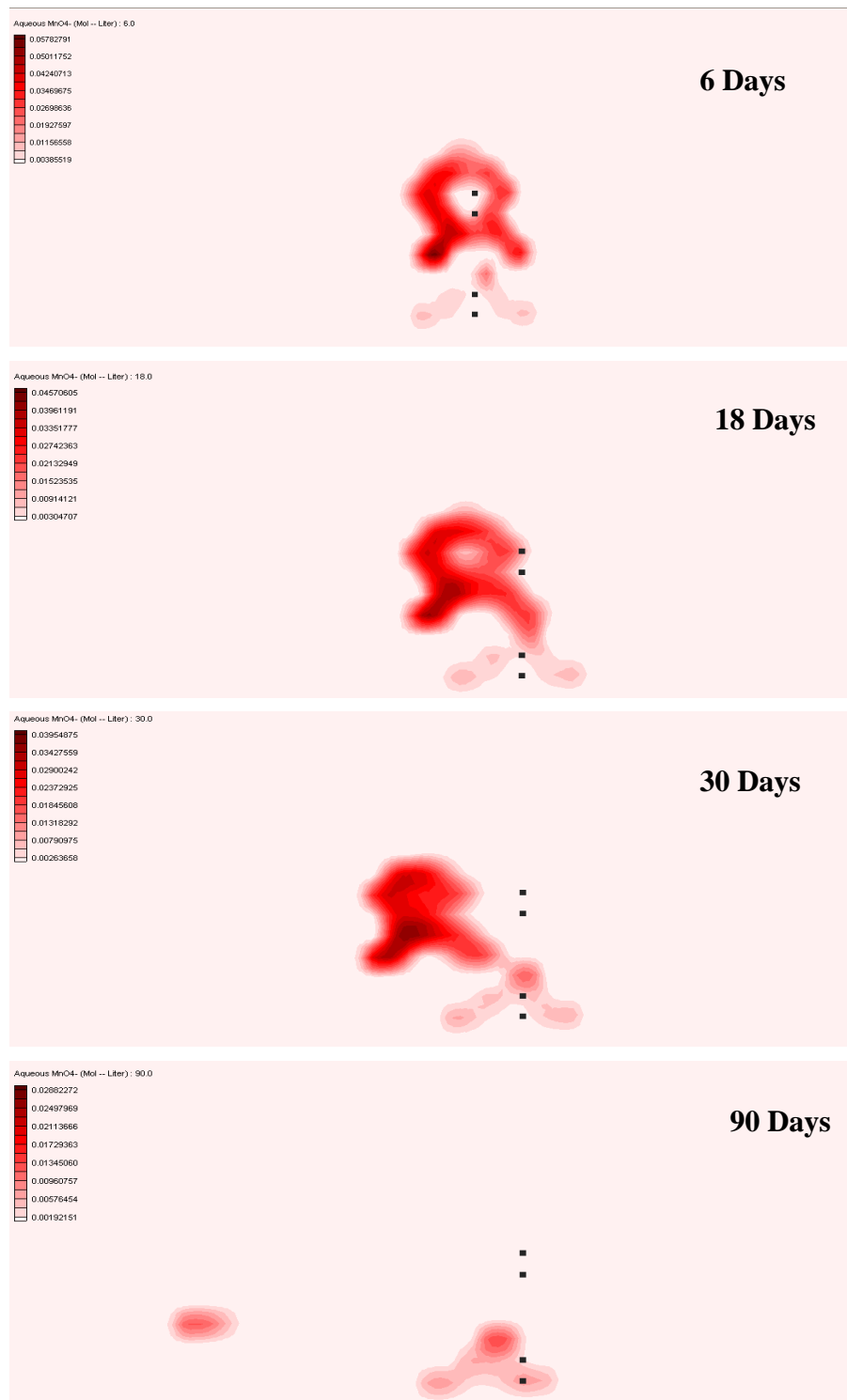


Figure 3-10b Profile View of Permanganate Distribution at 6, 18, 30 and 90 Days of Simulation with Scenario 4 (deep red indicate high concentration of permanganate)

An analysis was conducted to evaluate the sensitivity of the model simulation results to the NOD parameters. The pilot test was simulated using total NOD values equal to 10 and 100 times the scenario 4 values. Error statistics for this analysis are provided in **Table 3-8** for MnO₄. Statistics are only provided for permanganate since this parameter is thought to be a more important indicator of treatment. Increasing total NOD results in a lower RMSE. However, the fraction of wells matched decreases significantly.

Table 3-8 Error Statistics Comparing Simulated and Observed Permanganate Measurements with Increased Total NOD

| | MnO₄ | | | |
|-----------------|------------------------|--------------------|----------------|------------------|
| Scenario | RMSE | Not Matched | Matched | % Matched |
| 4 | 3.3E-03 | 18 | 85 | 83% |
| TNOD x10 | 3.09E-03 | 28 | 75 | 73% |
| TNOD x100 | 3.17E-03 | 30 | 73 | 71% |

3.6 Conclusion

A numerical model was developed to simulate the transport of MnO₄ through the aquifer at MMR and its reaction with TCE, NOD_I and NOD_S. Four scenarios were developed from kinetic parameters generated by batch NOD incubations. Each of these four scenarios provided an adequate match to MMR pilot test results.

CHAPTER 4 SENSITIVITY ANALYSIS

4.1 Introduction

Permanganate is most commonly injected in a grid configuration to treat contaminant source areas. This grid typically consists of several rows of wells with multiple wells installed in each row. In some cases, the spacing between rows is greater than spacing between wells within a row. This configuration is used when the ambient groundwater flow is used to enhance distribution of the permanganate. Once the target treatment zone has been defined, the designer must select a well spacing, mass of chemical reagent to inject, water injection volume, and injection sequence. Each of these parameters will influence contact efficiency (defined below). However, there is essentially no available information on the effect of these important design parameters on contact efficiency.

In this chapter, a series of numerical model simulations were conducted to evaluate the effect of important design parameters on contact efficiency. Model simulations were performed using the numerical modeling packages MODFLOW (McDonald and Harbaugh, 1988) and RT3D (Clement, 1997). Permanganate consumption and contaminant degradation are simulated using the modeling approach validated in Chapter 3.

4.2 Model Setup and Base Case Conditions

Figure 4-1 shows a hypothetical injection grid for area treatment of a 15 m x 15 m (approximately 50 ft x 50 ft) source area. The injection system consists of five rows of injection wells. Wells in each row are spaced 3 m (~ 10 ft) on-center and rows are spaced 3 m (~ 10 ft) apart. Alternating rows are offset with the objective of improving reagent distribution. Unfortunately, it is not practical to simulate this large area with a 3-dimensional heterogeneous permeability distribution. To reduce the computational burden, we have chosen to simulate a subsection of the treatment area shown by the dashed rectangle near the center of **Figure 4-1**. For a uniform grid, this subsection can be repeated over and over again to simulate the overall treatment area.

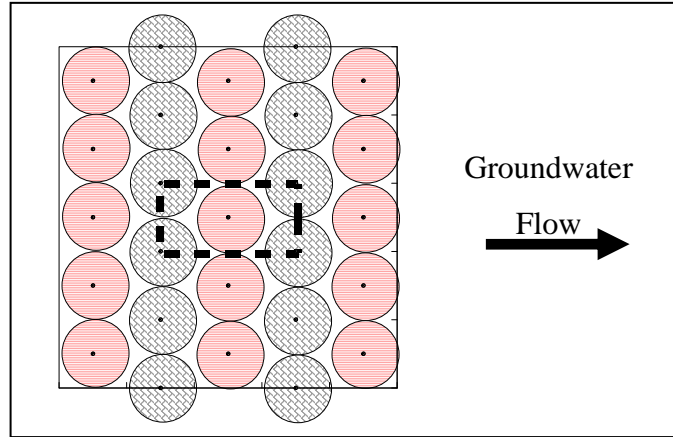


Figure 4-1 Hypothetical Injection Grid Showing Model Domain Subarea

Figure 4-2 shows an enlarged view of the model domain subsection. Standard conditions for the base case simulations are summarized in **Table 4-1**. Overall dimensions of the simulation grid are $3 S_y * S_x * Z$ where Z is the vertical thickness of the injection zone. Contaminant and permanganate transport were simulated with the Third order TVD scheme (ULTIMATE) within the RT3D numerical model. Dispersion was simulated with the GCG Package including the full dispersion tensor. Chemical reaction terms were solved using the 4th order Runge-Kutta solver. Grid discretization was $\Delta x = 0.25$, $\Delta y = 0.25$ m and $\Delta z = 0.05$ m resulting in a $13 * 73 * 60$ grid containing 56,160 cells. The background hydraulic gradient was established using constant head cells along the up-gradient and down-gradient boundaries of the grid. No flow boundaries are placed to simulate a recurring pattern of injection wells perpendicular to groundwater flow. The injection rate was 2 L/min per well ($2.88 \text{ m}^3/\text{d}$) for wells 1-4 and 4 L/min for well 5.

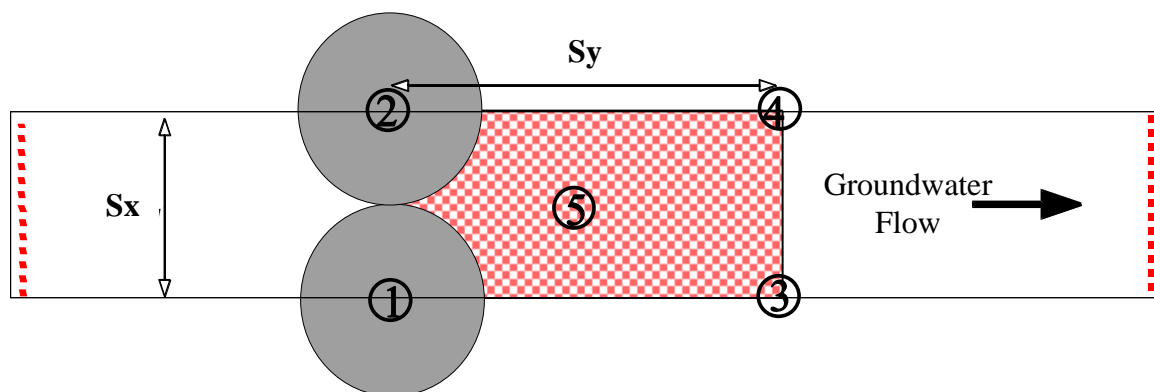


Figure 4-2 Model Domain for Numerical Simulations

Table 4-1 Base Case Simulation Conditions

| Parameter | Value | Units |
|---|----------------------|-----------------------------------|
| Well spacing perpendicular to flow (S_x) | 3 | m |
| Well spacing parallel to flow (S_y) | 6 | M |
| Vertical thickness of treatment zone (Z) | 3 | m |
| Effective porosity (n_e) | 0.2 | - |
| Bulk Density | 2000 | Kg m^{-3} |
| Longitudinal Dispersivity (α_L) | 0.01 | M |
| Transverse Dispersivity (α_T) | 0.001 | M |
| Vertical Dispersivity (α_v) | 0.0002 | M |
| Molecular diffusion coefficient | 1.7×10^{-5} | $\text{m}^2 \text{d}^{-1}$ |
| Stoichiometric coefficient ($Y_{M/C}$) | 1.33 | $\text{mol M (mol PCE)}^{-1}$ |
| Slow NOD reaction rate (k_{2S}) | 0.075 | $\text{L mol}^{-1} \text{d}^{-1}$ |
| Initial Contaminant Concentration | 7.61E-05 | mol PCE L^{-1} |
| Contaminant Retardation Factor (R_C) | 10 | - |
| Horizontal correlation length ($\lambda_x = \lambda_y$) | 2.0 | M |
| Vertical correlation length (λ_z) | 0.2 | M |
| Injection rate per well (Q) | 5.76 | $\text{m}^3 \text{d}^{-1}$ |
| Total NOD ($N_I + N_S$) | 0.04 | mol Kg^{-1} |
| Ratio Instantaneous NOD to Total NOD | 0.1 | mol Kg^{-1} |
| Permanganate Injection Concentration (M_I) | 0.4051 | mol L^{-1} |

The hydraulic conductivity field was represented as a spatially correlated random field with three levels of heterogeneity: (a) low; (b) moderate; and (c) high (**Table 4-2**). Five realizations of the permeability distribution were simulated for each level of heterogeneity. The realizations were generated using the turning bands method (Tompson et al., 1989) with a horizontal correlation length of 2 m and a vertical correlation length of 0.2 m. **Table 4-3** presents summary statistics for each realization.

Table 4-2 Characteristics for Low, Moderate, and High Levels of Heterogeneity

| Parameter | Low Heterogeneity | Moderate Heterogeneity | High Heterogeneity |
|--|-------------------|------------------------|--------------------|
| Average hydraulic conductivity (m/d) (K_{ave}) | 5 | 0.50 | 0.05 |
| Variance of $\ln K$ (σ^2) | 0.25 | 1.0 | 4.0 |
| Background (dh/dL) | 0.004 | 0.01 | 0.04 |
| Average Velocity (m/d) (V_{ave}) | 0.1 | 0.025 | 0.01 |

Table 4-3 Statistical Characteristics of Natural Log Transformed Hydraulic Conductivity Distributions used in Model Simulations

| | Mean | Variance |
|------------------------|-------|----------|
| Low Heterogeneity | | |
| Realization 1 (L1) | 5.997 | 0.220 |
| Realization 2 (L2) | 5.092 | 0.189 |
| Realization 3 (L3) | 5.528 | 0.282 |
| Realization 4 (L4) | 5.916 | 0.224 |
| Realization 5 (L5) | 5.913 | 0.296 |
| Moderate Heterogeneity | | |
| Realization 1 (M1) | 0.596 | 1.028 |
| Realization 2 (M2) | 0.810 | 0.879 |
| Realization 3 (M3) | 0.838 | 0.811 |
| Realization 4 (M4) | 1.016 | 0.984 |
| Realization 5 (M5) | 0.807 | 0.821 |

Table 4-3 Continued

| High Heterogeneity | | |
|--------------------|-------|-------|
| Realization 1 (H1) | 0.325 | 3.036 |
| Realization 2 (H2) | 0.192 | 3.211 |
| Realization 3 (H3) | 0.297 | 3.344 |
| Realization 4 (H4) | 0.555 | 4.374 |
| Realization 5 (H5) | 0.542 | 4.243 |

4.2.1 Scaling Factor

To allow easy comparison between different simulations, the mass of reagent injected and volume of fluid injected are presented as dimensionless scaling factors. The volume scaling factor (SF_V) for area treatment is the ratio of fluid (reagent plus water) injected to the pore volume of the target treatment zone where

$$SF_V = \text{Volume of water injected} / (n_e S_x S_y Z)$$

n_e is the effective porosity and Z is the effective saturated thickness. The mass scaling factor (SF_M) for area treatment is the ratio of reagent injected to the ultimate oxidant demand (UOD) of the target treatment zone where

$$SF_M = \text{MnO}_4 \text{ Mass injected} / (\text{UOD } \rho_B S_x S_y Z)$$

$$\text{UOD} = \text{NOD}_I + \text{NOD}_S + C * R_C * Y_{M/C} / \rho_B$$

and,

$$\text{NOD}_I = \text{Instantaneous NOD (mol Kg}^{-1}\text{)}$$

$$\text{NOD}_S = \text{Slow NOD (mol Kg}^{-1}\text{)}$$

$$\rho_B = \text{bulk density (Kg L}^{-1}\text{)}$$

$$C = \text{Average contaminant concentration in treatment zone (mol L}^{-1}\text{)}$$

$$R_C = \text{linear equilibrium retardation factor of the contaminant}$$

$$Y_{M/C} = \text{molar ratio of M to C consumed (moles/mol)}$$

For the base case simulations, $NOD_I = 0.004 \text{ mol Kg}^{-1}$, $NOD_S = 0.036 \text{ mol Kg}^{-1}$, the target contaminant (PCE) concentration was set to $7.61 \times 10^{-5} \text{ mol L}^{-1}$ (12,620 $\mu\text{g/L}$) with $R_C = 10$. For $SF_M = 1.0$, the amount of permanganate injected was 4320 mol (683 Kg of potassium permanganate) or 1080 mol (85 Kg) per well for well 1-4 and 2160 mol (341 Kg) for well 5. However, since half of oxidants injected to well 1-4 migrates outside of the target area (white area in **Figure 4-2**), only half (540 mol) of the permanganate injected into wells 1 -4 is included in the SF_M calculation.

4.2.2 Typical Simulation Results

Figure 4-3 and **4-4** show the hydraulic conductivity, M , NOD_I , NOD_S , C distributions in both plan (**Figure 4-3**) and longitudinal cross-section (**Figure 4-4**) when M is injected into wells 1-5 with $SF_V = SF_M = 0.25$ at 120 days after the start of injection. The dark red indicates higher values for that parameter, while light pink or white indicates lower values. In these simulations, the wells are injected sequentially (from 1 to 5) and the aquifer was assumed to be moderately heterogeneous (permeability realization #3). For $SF_V = SF_M = 0.25$, sufficient water is injected to fully saturate 25% of the pore space within the treatment zone and consume 25% of the ultimate oxidant demand within the treatment zone.

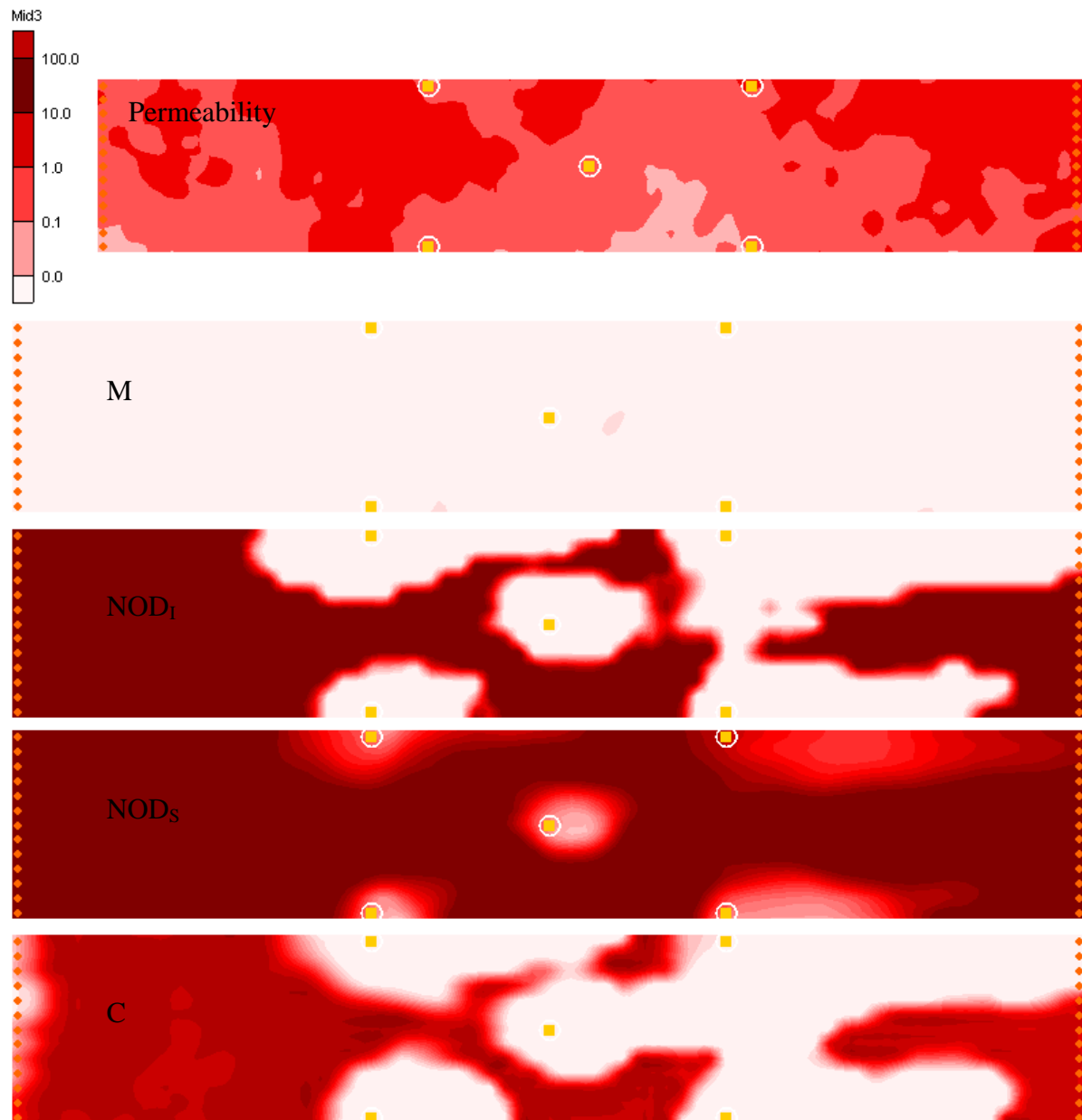


Figure 4-3 Horizontal Hydraulic Conductivity, Permanganate (M), NOD_I , NOD_S and Contaminant Distribution (C) in Top Layer of Aquifer (see Figure 4-4) (with moderately heterogeneous aquifer (realization #3), wells 1-5 are injected with $SF_V = SF_M = 0.25$)

In plan view (**Figure 4-3**), the distribution of permanganate appears to be controlled by the location of the injection points, permeability distribution, and ambient groundwater flow. Initially, the highest permanganate concentrations

develop near the injection wells. Once injection is complete, permanganate migrates down-gradient, preferentially migrating through the higher permeability zones. By 120 days, permanganate (M) concentrations are low throughout the simulation domain due to reaction with contaminants (C) and NOD, and down-gradient transport. NOD_I is depleted (indicated by white) in any area contacted by M. C is also depleted in these areas. However, the C depleted zones appear to be slightly larger with more diffuse boundaries than the NOD_I depleted zones, presumably due to transport of dissolved C into areas containing M. The areas where NOD_S is depleted are much smaller than the NOD_I and C depleted areas, indicating substantial amounts of NOD_S remain in areas that were temporarily contacted by M.

In profile view (**Figure 4-4**), the effects of a heterogeneous permeability distribution on M transport are very apparent. In high permeability layers, M migrates rapidly down-gradient resulting in complete depletion of NOD_I from these layers. As in plan view, the C depleted zones appear to be slightly larger than the NOD_I depleted zones, presumably due to transport of C from untreated areas into zones with residual M. NOD_S depleted zones are much smaller than the NOD_I depleted zones indicating significant amounts of NOD_S remain in zones that were at least temporarily contacted by M.

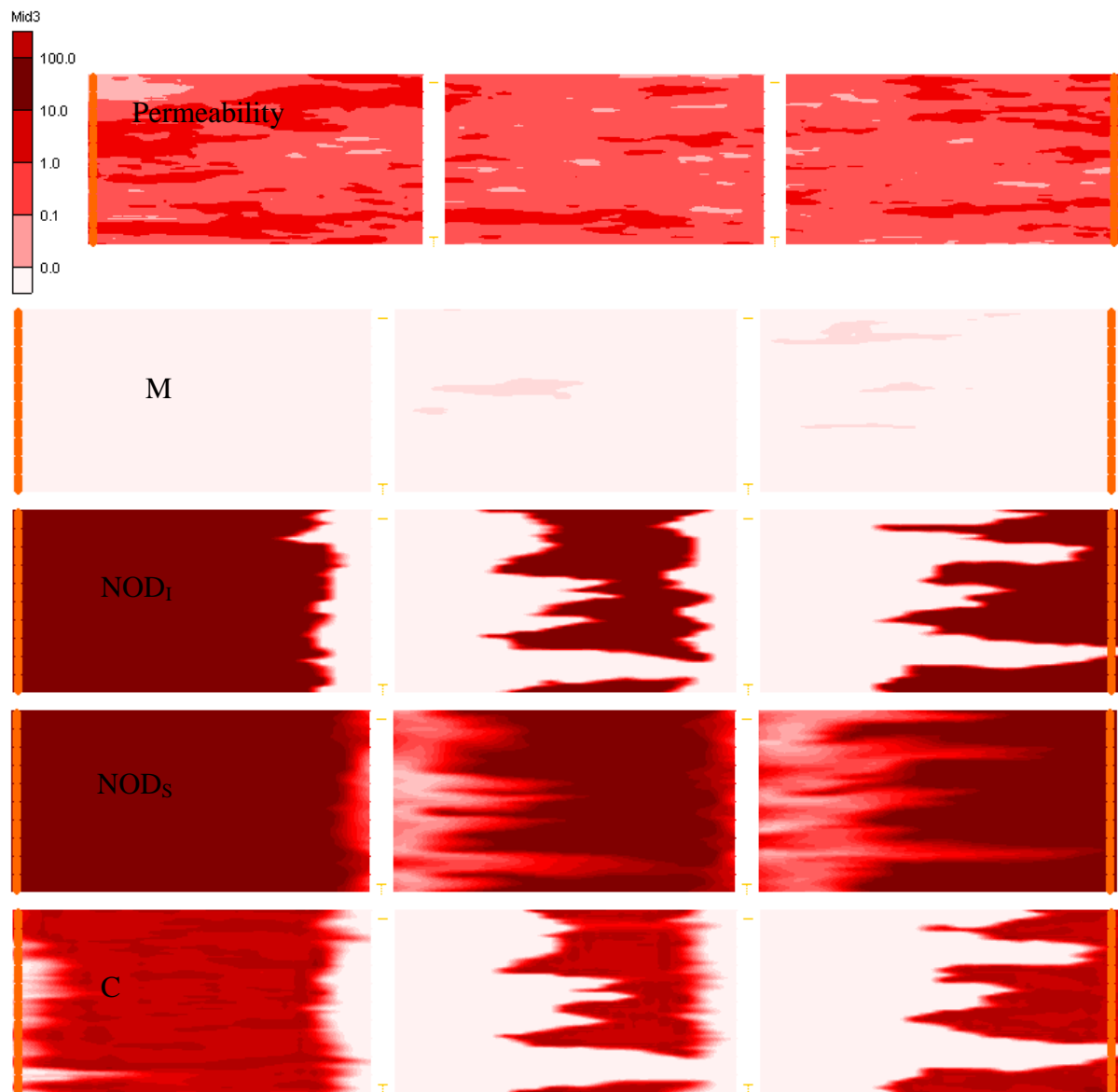


Figure 4-4 Vertical Hydraulic Conductivity, Permanganate (M), NOD_I, NOD_S and Contaminant Distribution (C) in Last Row of Aquifer (bottom row of Figure 4-3) (with moderately heterogeneous aquifer (realization #1), wells 1-5 are injected with $SF_V = SF_M = 0.25$)

The numerical model simulations indicate that permanganate injection would be effective in destroying contaminants in substantial portions of the simulation domain. However, significant portions of the model domain were not contacted with M and consequently, large amounts of C remain untreated. Over time, this untreated

contaminant will migrate down-gradient resulting in an apparent rebound in contaminant concentrations. Very high contact efficiencies will be required to reach target cleanup standards at many sites. In subsequent sections, sensitivity analyses will be conducted to examine the effect of different parameters on contact efficiency. This information can be used to generate improved designs with higher contact efficiencies.

4.2.3 Criteria for Determining Contact Efficiency

Ideally, we would like to uniformly distribute permanganate throughout the entire treatment zone. However, spatial variations in hydraulic gradient and hydraulic conductivity result in a heterogeneous permanganate distribution and less than desired treatment efficiency. Simulation results presented in subsequent sections will show that permanganate distribution and resulting treatment efficiency can be enhanced by modifying the injection approach. However, modifying the injection approach will also increase costs. Quantitative measures of the distribution efficiency are needed to evaluate the relative benefits of alternative injection approaches.

In this work, we will examine two different measures of contact and treatment efficiency. The first is the Aquifer Volume Contact Efficiency (E_V) where

$$E_V = \frac{\text{volume of treatment zone where } \text{NOD}_I \text{ is reduced by over 90\%}}{\text{total volume of treatment zone}}$$

The second is the Contaminant Mass Treatment Efficiency (E_M)

$$E_M = \frac{\text{volume of treatment zone where over 90\% of contaminant is removed}}{\text{total volume of treatment zone}}$$

Both E_V and E_M are evaluated at 120 days after injection for the target treatment zone, defined as the region between the 1st and 3rd rows of injection wells (shaded area) in **Figure 4-2**. A MATLAB procedure was developed to query to model simulation results and generate statistics for E_V and E_M .

4.3 Effect of Fluid Volume, Permanganate Mass and Time on Treatment Efficiency

An initial set of simulations were conducted to examine the effect of injection fluid volume, permanganate mass, and time on treatment efficiency. In these simulations, a simpler configuration where only wells 1 -4 were injected (well #5 was not activated). Variations in the mass of M and volume of water injected are represented by changes in Mass and Volume Scaling Factors (SF_M and SF_V). In these simulations, mass of M and fluid volume were varied to generate values of SF_M and SF_V equal to 0.05, 0.125, 0.25, 0.375, 0.5, 0.75 and 1.

Figure 4-5a and **4-5b** show how aquifer volume contact efficiency (E_V) and pollutant mass contact efficiency (E_M) vary over time following injection of different amounts of M (represented by variations in SF_M). For all the simulation results presented in **Figure 4-5a** and **4-5b**, injection volume is held constant ($SF_V=0.25$). These simulations are equivalent to varying the permanganate concentration while keeping the injection volume constant.

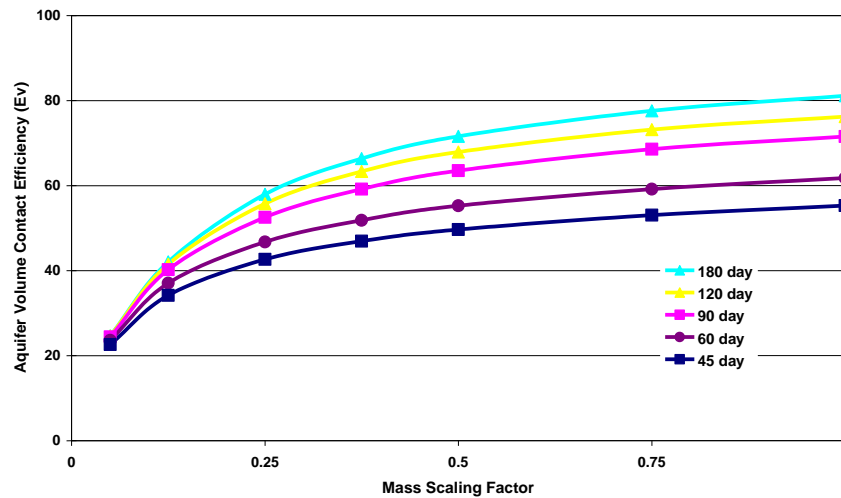


Figure 4-5a Variation in Aquifer Volume Contact Efficiency (E_V) with Time where Fluid Injection Volume is held Constant ($SF_V=0.25$) and Permanganate Mass Varies (SF_M varies from 0.05 to 1.0))

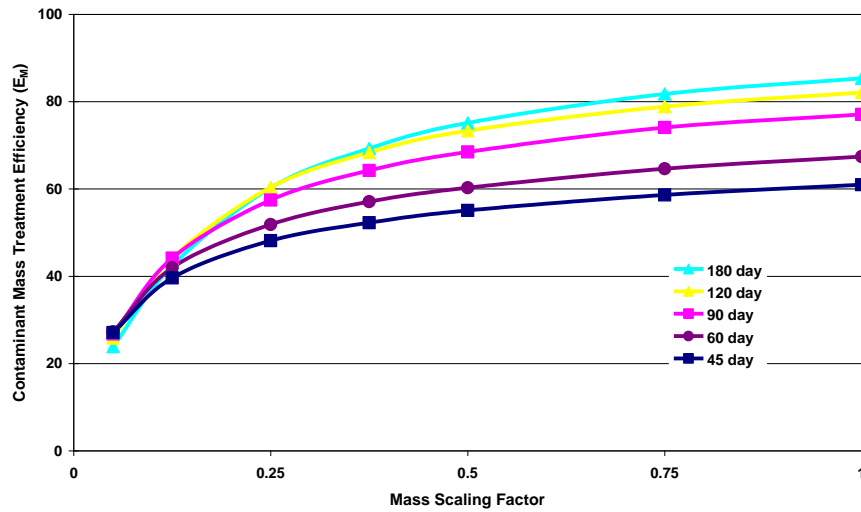


Figure 4-5b Variation in Contaminant Mass Treatment Efficiency (E_M) with Time where Fluid Injection Volume is held Constant ($SF_V=0.25$) and Permanganate Mass Varies (SF_M varies from 0.05 to 1.0))

For small amounts of M injected ($SF_M < 0.125$), the M is rapidly consumed, and both E_V and E_M remain constant over time. However, when greater amounts of M are injected ($SF_M > 0.25$), E_V and E_M increase gradually with time, presumably due to down-gradient migration / dispersion of dissolved M. The increase in contact efficiency with time is greatest for the highest values of SF_M , since larger amounts of M would last the longest, allowing for the greatest drift/dispersion.

Overall, the trends in E_V (Figure 4-5a) and E_M (Figure 4-5b) are similar. However, E_M (pollutant mass removal efficiency) is slightly greater than E_V (aquifer volume contact efficiency) since dissolved contaminants can migrate from untreated high concentration zones to permanganate contacted zones where the contaminant concentration is zero.

Figure 4-6a and **4-6b** illustrate how E_V and E_M vary over time following injection of different amounts of fluid while keeping the M concentration constant ($SF_V = SF_M$). When both SF_V and SF_M are increased, the permanganate is rapidly distributed throughout the treatment zone, resulting in more rapid initial treatment. As a consequence, the differences in treatment efficiency at 30 days and 180 days are

less pronounced. The overall trends in E_V (Figure 4-6a) and E_M (Figure 4-6b) are similar (as observed in Figure 4-5a and Figure 4-5b), suggesting that tracking both E_V and E_M is unnecessary. For the remainder of this report, only results for E_M will be presented.

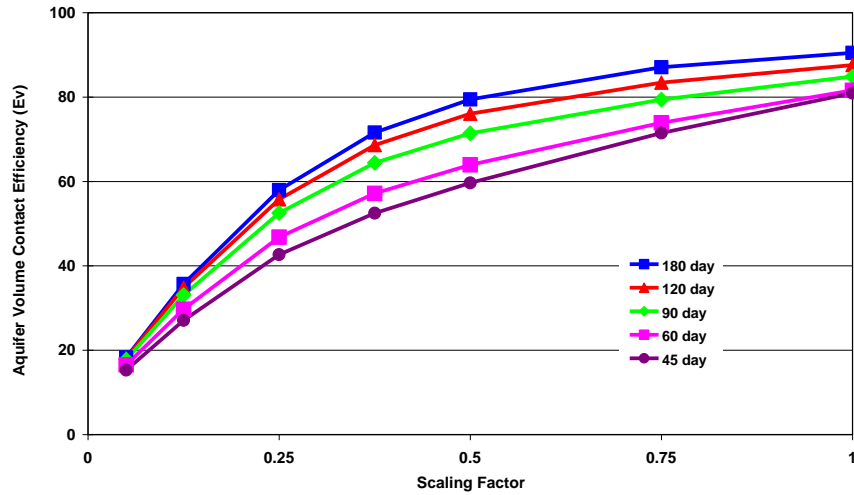


Figure 4-6a Variation in Aquifer Volume Contact Efficiency (E_V) with Time where Permanganate Concentration is held Constant ($SF_V = SF_M$) and the Volume of the Permanganate Injection Solution Varies (both SF_V and SF_M varies from 0.05 to 1.0)

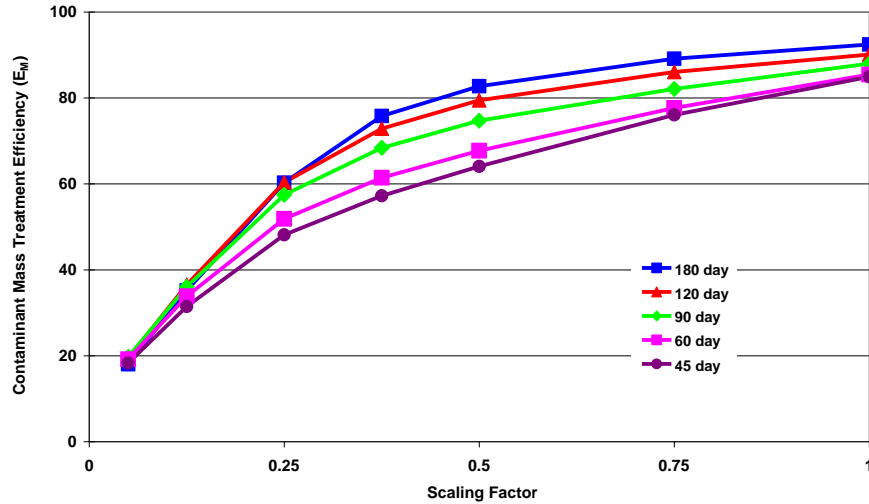


Figure 4-6b Variation in Contaminant Mass Treatment Efficiency (E_M) with Time where Permanganate Concentration is held Constant ($SF_V = SF_M$) and the Volume of the Permanganate Injection Solution Varies (both SF_V and SF_M varies from 0.05 to 1.0)

Figure 4-7 presents results showing the effect on E_M at 180 days for the following conditions: (a) varying permanganate mass (varying SF_M) while keeping fluid volume constant ($SF_V = 0.25$), (b) varying fluid volume (varying SF_V) while keeping permanganate mass constant ($SF_M = 0.25$), and (c) varying both permanganate mass and fluid volume (vary both SF_V and SF_M) while keeping permanganate concentration constant ($SF_V = SF_M$). For constant permanganate mass ($SF_M = 0.25$), increasing fluid volume injected (increasing SF_V) initially results in an improvement in E_M . However, further increases in SF_V beyond 0.375 result in little additional benefit. This trend is presumably due to the rapid consumption in permanganate when a relatively small amount of reagent is injected. Conversely, when fluid volume is held constant ($SF_V = 0.25$), increasing permanganate mass injected (increasing SF_M) results in a continuous increase in E_M . This trend is presumably due to down-gradient drift/dispersion of permanganate when larger amounts of reagent are injected. The best performance occurs when both SF_V and SF_M are increased. Injecting larger amounts of water (increasing SF_V) result in more rapid distribution of the permanganate, improving contact with the contaminant and reducing waste of M by

reaction with NOD_S . Injecting more permanganate (increasing SF_M) allows the permanganate to last longer, providing more time for contaminants to diffuse out of lower permeability zones.

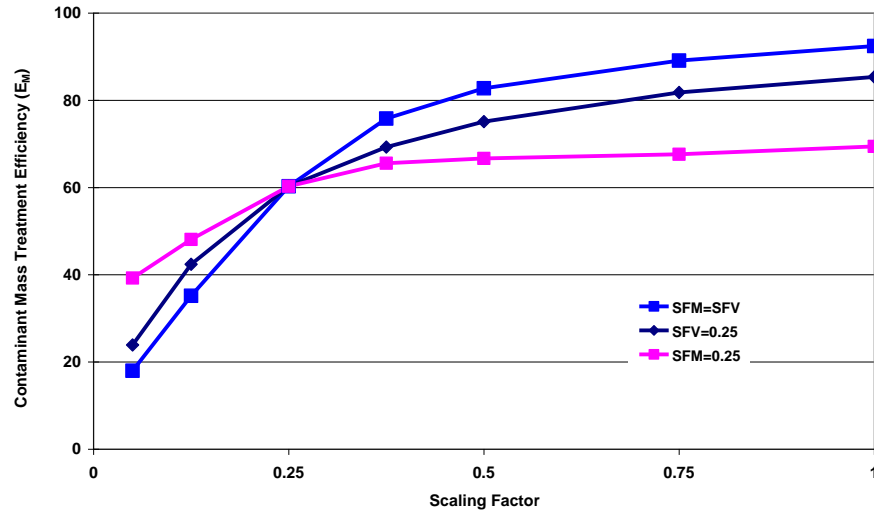


Figure 4-7 Variation in Contaminant Mass Treatment Efficiency (E_M) at 180 days after Injection with Mass and Volume Scaling Factors

Overall, treatment efficiency appears to be best when $\text{SF}_M = \text{SF}_V$. This approach will be used in subsequent sensitivity analyses examining the effect of different parameters on E_M .

4.4 Sensitivity Analyses

A series of sensitivity analyses were conducted to examine the effect of model input parameters on treatment efficiency. The parameters expected to have the greatest impact on treatment efficiency are thought to be: (1) the Slow NOD reaction rate (k_{2S}); (2) the Total NOD ($N_I + N_S$); (3) the ratio of NOD_I to Total NOD; (4) the initial contaminant concentration; (5) the contaminant retardation factor (R); and (6) the level of heterogeneity. **Table 4-4** shows the parameter values used the sensitivity

analyses. As in section 4.3, simulations were run with SF_M and SF_V equal to 0.05, 0.125, 0.25, 0.375, 0.5, 0.75, and 1.

Table 4-4 Input Parameters used in Sensitivity Analyses Simulations

| | Ratio to Base | Initial C | Total NOD | NOD _I | k_{2S} | Fraction NOD _I | R | M Injection Conc. | K _{ave} | Hydraulic Gradient (dh/dL) | V _{ave} |
|--------------------------------|---------------|-------------------|--------------|------------------|---------------|---------------------------|------------|-------------------|------------------|----------------------------|------------------|
| | | mol/L | Mol/kg | mol/kg | L/mol-day | % | - | mol/L | m/day | - | m/day |
| Slow reaction rate | 0.1 | 0.0000761 | 0.04 | 0.004 | 0.0075 | 10 | 10 | 0.40506 | 0.5 | 0.01 | 0.025 |
| | 1 | 0.0000761 | 0.04 | 0.004 | 0.075 | 10 | 10 | 0.40506 | 0.5 | 0.01 | 0.025 |
| | 10 | 0.0000761 | 0.04 | 0.004 | 0.75 | 10 | 10 | 0.40506 | 0.5 | 0.01 | 0.025 |
| Total NOD | 0.1 | 0.0000761 | 0.004 | 0.0004 | 0.075 | 10 | 10 | 0.04506 | 0.5 | 0.01 | 0.025 |
| | 1 | 0.0000761 | 0.04 | 0.004 | 0.075 | 10 | 10 | 0.40506 | 0.5 | 0.01 | 0.025 |
| | 10 | 0.0000761 | 0.4 | 0.04 | 0.075 | 10 | 10 | 4.00506 | 0.5 | 0.01 | 0.025 |
| Instantaneous NOD ratio | 0.05 | 0.0000761 | 0.04 | 0.002 | 0.075 | 5 | 10 | 0.40506 | 0.5 | 0.01 | 0.025 |
| | 1 | 0.0000761 | 0.04 | 0.004 | 0.075 | 10 | 10 | 0.40506 | 0.5 | 0.01 | 0.025 |
| | 0.2 | 0.0000761 | 0.04 | 0.008 | 0.075 | 20 | 10 | 0.40506 | 0.5 | 0.01 | 0.025 |
| Initial Contaminant | 0.1 | 0.00000761 | 0.04 | 0.004 | 0.075 | 10 | 10 | 0.40051 | 0.5 | 0.01 | 0.025 |
| | 1 | 0.0000761 | 0.04 | 0.004 | 0.075 | 10 | 10 | 0.40506 | 0.5 | 0.01 | 0.025 |
| | 10 | 0.000761 | 0.04 | 0.004 | 0.075 | 10 | 10 | 0.45061 | 0.5 | 0.01 | 0.025 |
| Retardation Factor | 1 | 0.0000761 | 0.04 | 0.004 | 0.075 | 10 | 1 | 0.40051 | 0.5 | 0.01 | 0.025 |
| | 10 | 0.0000761 | 0.04 | 0.004 | 0.075 | 10 | 10 | 0.40506 | 0.5 | 0.01 | 0.025 |
| | 100 | 0.0000761 | 0.04 | 0.004 | 0.075 | 10 | 100 | 0.45061 | 0.5 | 0.01 | 0.025 |
| Heterogeneity Level | LOW | 0.0000761 | 0.04 | 0.004 | 0.075 | 10 | 10 | 0.40506 | 5 | 0.004 | 0.1 |
| | MID | 0.0000761 | 0.04 | 0.004 | 0.075 | 10 | 10 | 0.40506 | 0.5 | 0.01 | 0.025 |
| | HIGH | 0.0000761 | 0.04 | 0.004 | 0.075 | 10 | 10 | 0.40506 | 0.05 | 0.04 | 0.01 |

4.4.1 Effect of Slow NOD Reaction Rate on E_M

Figure 4-8 shows the effect of varying the slow NOD reaction rate (k_{2S}) by a factor of ten on E_M when the SF_M and SF_V both vary from 0.05 to 1. A higher value of k_{2S} reduces contact efficiency because the permanganate is more rapidly consumed.

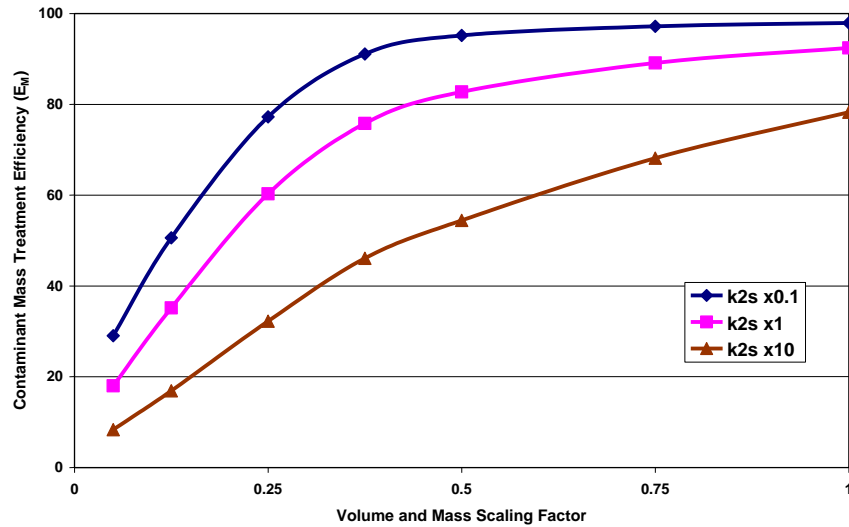


Figure 4-8 Effect of Slow NOD Reaction Rate (k_{2S}) on E_M at 180 days ($SF_V = SF_M$)

4.4.2 Effect of Total NOD on E_M

Figure 4-9 shows the effect of varying the total NOD of the aquifer material by a factor of ten on E_M when the SF_M and SF_V vary from 0.05 to 1. Our initial assumption was that the absolute value of Total NOD would have little effect on E_M for a constant value of SF_M , since a factor of ten increases in total NOD would also result in a factor of ten increases in mass of permanganate injected. This assumption was clearly not correct. Increasing total NOD significantly reduces E_M .

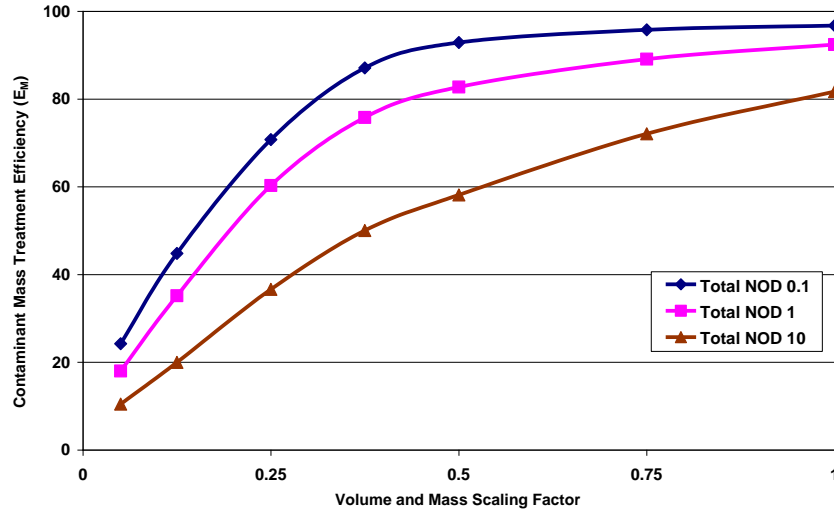


Figure 4-9 Effect of Total NOD on E_M at 180 days ($SF_V=S F_M$)

It appears that the reduction in E_M with increasing total NOD results from the increased rate of reaction between NOD and M. Equation 4-1 shows the 2nd order relationship used to describe the rate of M depletion by reaction with slow NOD (N_S).

$$\frac{dM}{dt} = -\rho_B k_{2S} N_S M / n \quad (4-1)$$

The effective first order decay rate for M is $\rho_B k_{2S} N_S / n$. Increasing the absolute value of NOD_S by a factor of ten increases the effective decay rate by a factor of ten, similar to an increase in k_{2S} . This explains the apparent similarity in **Figure 4-8** and **Figure 4-9**. The decline in E_M with increasing k_{2S} and increasing total NOD, both appear to be due to an increase in the rate of reaction between M and NOD_S . This effect is illustrated in **Figure 4-10** where data from **Figure 4-8** and **4-9** are plotted together. Increasing total NOD by a factor of ten has a similar effect to increasing k_{2S} by a factor of ten. However, the impact of increasing total NOD is somewhat less because as the reaction between M and NOD proceeds, NOD becomes depleted and the reaction slows.

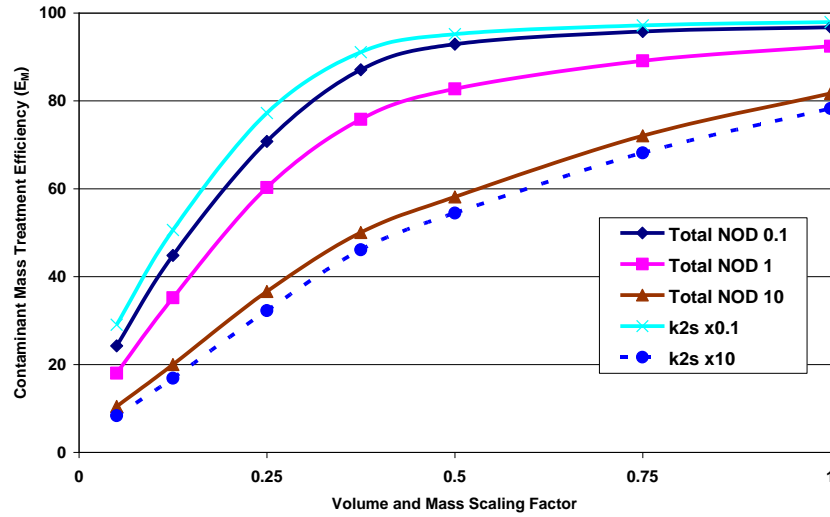


Figure 4-10 Effect of Slow NOD Reaction Rate (k_{2s}) and Total NOD on E_M at 180 days ($SF_V = SF_M$)

4.4.3 Effect of NOD_I on E_M

Figure 4-11 shows the effect of varying the instantaneous fraction of NOD by a factor of two on E_M when the SF_M and SF_V vary from 0.05 to 1. For a constant value of total NOD, varying the fraction instantaneous is equivalent to varying NOD_I . Increasing the instantaneous fraction reduced E_M , due to the more rapid consumption of M. However, the effect on E_M is somewhat less than shown in **Figure 4-8** and **4-9**, presumably due to the smaller range of values examined in this sensitivity analysis. The smaller range examined here is based on values reported in the published literature.

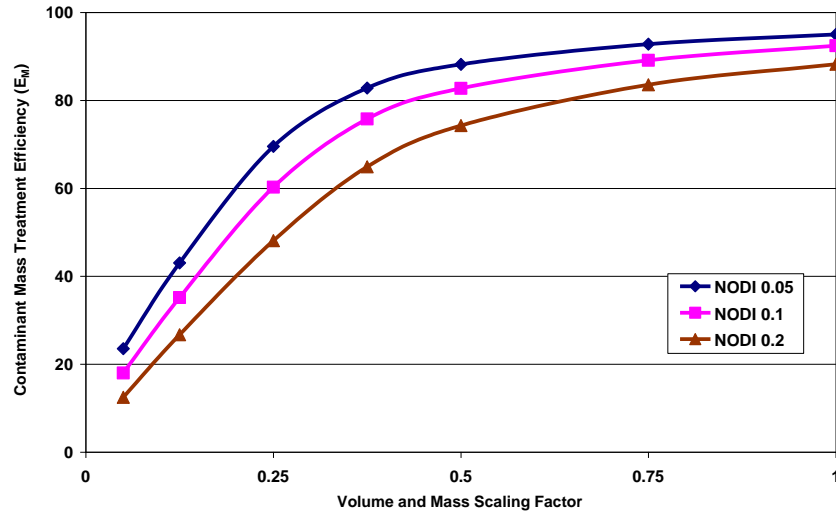


Figure 4-11 Effect of Fraction NOD_I on E_M at 180 days ($SF_V = SF_M$)

4.4.4 Effect of Initial Contaminant Concentration and Contaminant Retardation Factor on E_M

Figure 4-12 and **4-13** show the effect of varying the initial contaminant concentration and contaminant retardation factor on E_M . Both factors had a relatively minor impact on E_M . This is presumably due to the relatively small amount of permanganate consumed during reaction with the contaminant in comparison to that consumed by NOD.

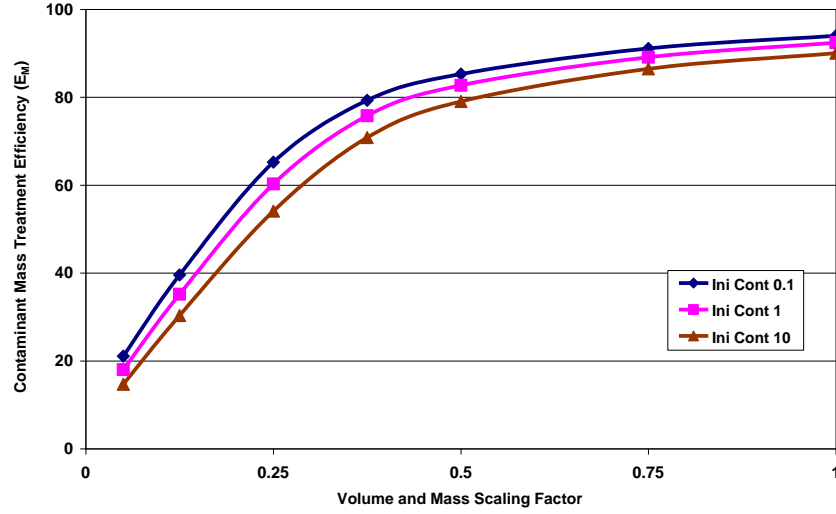


Figure 4-12 Effect of Initial Contaminant Concentration on E_M at 180 days ($SF_V = SF_M$)

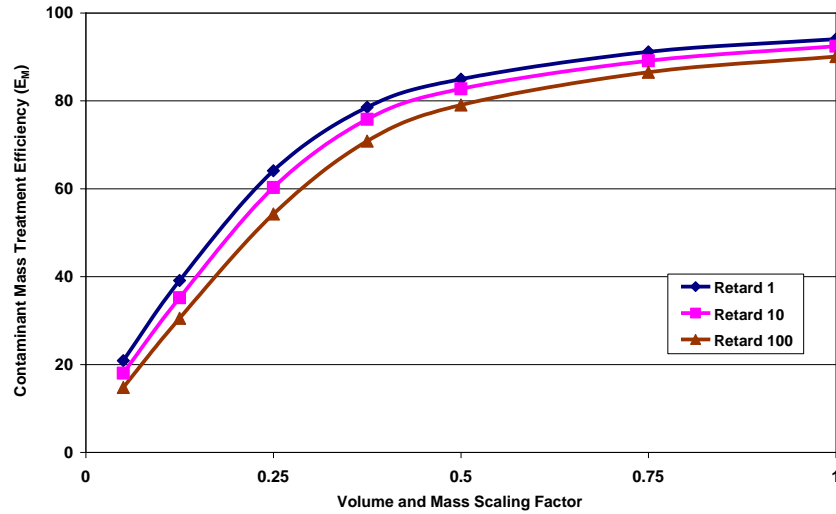


Figure 4-13 Effect of Retardation Factor on E_M at 180 days ($SF_V = SF_M$)

4.4.5 Effect of Aquifer Heterogeneity on E_M

Figure 4-14 shows the effect of varying the level of aquifer heterogeneity on E_M when the SF_M and SF_V vary from 0.05 to 1. The error bars show the standard deviation of E_M values obtained for the five different realizations simulated for each level of heterogeneity (see **Table 4-2** and **4-3**). For volume and mass scaling factors (SF_V and SF_M) less than 0.5, the medium and high heterogeneity distributions result in a somewhat

higher contact efficiency than the low heterogeneity distribution. It may be that the presence of higher permeability channels results in more rapid transport of permanganate away from the injection well when only a small amount of fluid is injected. Once injected, the permanganate can then migrate into medium permeability zones, treating some additional contaminants. However for SF_V and SF_M greater than 0.5, the situation is reversed. When aquifer heterogeneity is medium or high, permanganate cannot penetrate the lower permeability zones, reducing the maximum level of treatment that can be achieved.

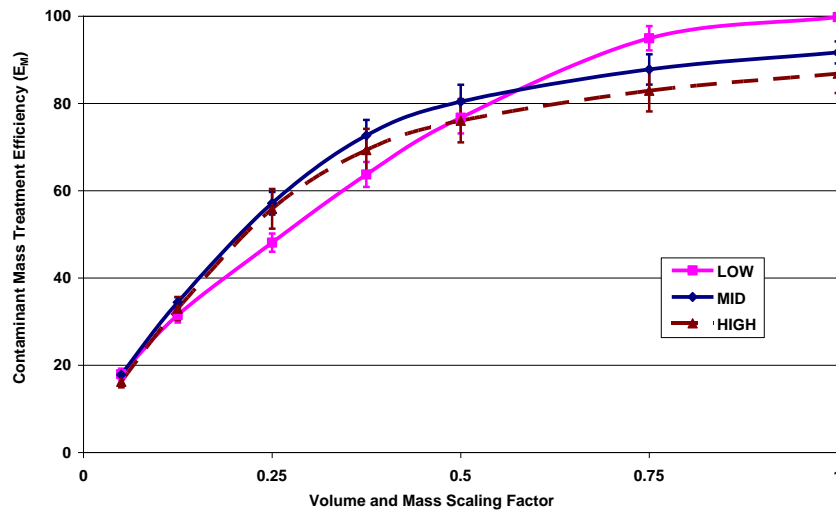


Figure 4-14 Effect of Aquifer Heterogeneity on E_M at 180 days ($SF_V = SF_M$) (error bars show the standard deviation in E_M observed in five permeability realizations for each level of heterogeneity)

CHAPTER 5 SUMMARY AND CONCLUSIONS

The objective of this research is to develop information that can be used to improve the performance of injection systems for distributing permanganate in contaminated aquifers. Results of this research are summarized below.

1. Six different kinetic relationships were examined to identify the relationship that best fits the loss of permanganate in experimental incubations using soil C from MMR. The three models that included a 2nd order relationship between permanganate concentration (M) and NOD concentration all provided an equally good fit to the experimental data. Model 6 was selected for future use based on its' ability to fit the experimental data, ease of numerical solution, and flexibility in simulating NOD composed of rapidly and slowly reactive materials. Model 6 includes a fraction of NOD which instantaneously reacts with M and a slow NOD component which reacts with M by a 2nd order relationship.
2. The numerical model RT3D was modified to simulate ISCO treatment by developing a module that simulates reactions between permanganate, NOD and contaminants. The reaction between permanganate and a single contaminant is simulated as an instantaneous reaction. The reaction between permanganate and NOD is simulated using Model 6 previously developed.
3. The newly developed RT3D model was used to simulate an ISCO pilot test at MMR conducted in fall 2007. Kinetic parameters used to calibrate the model were estimated from prior laboratory tests. The new model provided an adequate match to the field data demonstrating this approach is appropriate for simulating ISCO of groundwater contaminants.
4. The validated model was then applied to a hypothetical heterogeneous aquifer to evaluate the effect of different design variables and aquifer parameters on treatment efficiency. A series of sensitivity analyses generated the following results.
 - a. When small amounts of permanganate are injected, the reagent is rapidly consumed and pollutant removal efficiency does not increase with time after

the first 30 days. However, when larger amounts of permanganate are injected, the reagent can persist for several months resulting in a gradual increase in treatment efficiency with time.

- b. For constant permanganate mass, increasing fluid volume injected initially results in an improvement in treatment efficiency. However, further increases in fluid volume injected result in little additional benefit. Conversely, when fluid volume is held constant and permanganate mass is increased, treatment efficiency steadily increases, presumably due to down-gradient drift/dispersion of permanganate when larger amounts of reagent are injected. The highest treatment efficiencies are obtained when both fluid volume and permanganate mass are increased.
- c. Higher values of the slow NOD reaction rate reduce contact efficiency because the permanganate is more rapidly consumed.
- d. Higher values of total NOD reduce contact efficiency, even when proportionally more permanganate is injected due to the higher reaction rate that results.
- e. Increasing the instantaneous NOD fraction reduces treatment efficiency somewhat.
- f. Changes in the initial contaminant concentration and contaminant retardation factor have a relatively minor impact on treatment efficiency.
- g. When small amounts of fluid and permanganate are injected, moderate to high levels of heterogeneity may actually increase treatment efficiency, by causing more rapid transport of permanganate away from the injection point. However, when larger amounts of water and permanganate are injected, moderate to high heterogeneity reduces treatment efficiency since the reagent cannot penetrate the lower permeability zones.

REFERENCES

AFCEE, (2007a) The Installation Restoration Program at the Massachusetts Military Reservation (MMR), Air Force Center for Engineering and the Environment <http://mmr.org/>

AFCEE, (2007b) Groundwater Plume Maps and Information Booklet, Air Force Center for Engineering and the Environment

ATSDR, (2004) Medical Management Guidelines for Tetrachloroethylene, Agency for Toxic Substances and Disease Registry, Division of Toxicology and Environmental Medicine, US

ATSDR, (2007) CERCLA Priority List of Hazardous Substances that will be The Subject of Toxicological Profiles and Support Document, Agency for Toxic Substances and Disease Registry, Division of Toxicology and Environmental Medicine, US

ASTM D7262, (2007) Standard Test Method for Estimating the Permanganate Natural Oxidant Demand of Soil and Aquifer Solids, In; ASTM International: West Conshohocken, PA

CH2MHILL, (2007) Project Note for CS-10 ISCO Pilot Test Work Plan

Chambers, J.D., Leavitt, A.L., Walti, C.L., Schreier, C.G., Melby, J.T., and Goldstein, L., (2000) Treatability Study – Fate of Chromium during Oxidation of Chlorinated Solvents, In: Proceedings of International Conference on Remediation of Chlorinated and Recalcitrant Compounds, Columbus, OH, pp. 57-66

Clement, T.P., (1997) RT3D: A Modular Computer Code for Simulation of Reactive Multispecies Transport in 3-Dimensional Groundwater Systems, US Department of Energy

Drescher, E.A., Gavaskar, R., Sass, B.M., Cumming, L.J., Drescher, M.J., and Williamson, T., (1999) Batch and Column Testing to Evaluate Chemical Oxidation of DNAPL Source Areas, In: Proceeding of International Conference on Remediation of Chlorinated and Recalcitrant Compounds, Columbus, OH, pp. 425-432

Eilbeck, W.J., and Mattock, G., (1987) Chemical Processes in Wastewater Treatment, John Wiley and Sons, Toronto, Ontario

Gates, D.D., Siegrist, R.L., and Cline, S.R., (1995) Chemical Oxidation of Volatile and semi-Volatile Organic Compounds in Soil, US, pg. 17

Gates, D.D., Siegrist, R.L., and Cline, S.R., (2001) Comparison of Potassium Permanganate and Hydrogen Peroxide as Chemical Oxidants for Organically Contaminated Soils, Journal of Environmental Engineering 127(4), pp. 337-347

Harbaugh, A.W., Banta, E.R., Hill, M.C., and McDonald, M.G., (2000) MODFLOW-2000, the US Geological Survey Modular Ground-Water Model - User Guide to Modularization Concepts and the Ground-Water Flow Process, Open-File Report 00-92, US Geological Survey, pg. 121

Haselow, J.S., Siegrist, R.L., Crimi, M., and Jarosch, T., (2003) Estimating the Total Oxidant Demand for In Situ Chemical Oxidation Design, Remediation Journal 13(4), pp. 5-16

Hood, E.D., (2000a) Permanganate Flushing of DNAPL Source Zones: Experimental and Numerical Investigation, Civil and Environmental Engineering, Waterloo, University of Waterloo, PhD Dissertation

Hood, E.D., and Thomson N.R., (2000b) Numerical Simulation of In Situ Chemical Oxidation, In: Proceedings of International Conference on Remediation of Chlorinated and Recalcitrant Compounds, Columbus, OH, pp. 82-90

Huling, S.G., and Pivetz, B.E., (2006) In-Situ Chemical Oxidation - Engineering Issue, US Environmental Protection Agency, National Risk Management Research Laboratory, R.S. Kerr Environmental Research Center, Ada, OK, EPA 600-R-06-072

Hutson, S.S., (2004) Estimated Use of Water in the United States in 2000, US Geological Survey, Reston, VA

Jones, L.J., (2007) The Impact of NOD Reaction Kinetic on Treatment Efficiency, Civil and Environmental Engineering, Waterloo, University of Waterloo, MS Thesis

Leung, S.W., Watts, R.J., and Miller, G.C., (1992) Degradation of Perchloroethylene by Fenton's Reagent: Speciation and Pathway, *Journal of Environmental Quality* 21, pp. 377-381

Lowe, K.S., Gardner, F.G., Siegrist R.L., and Houk T.C., (1999) Field Pilot Test of In Situ Chemical Oxidation Through Recirculation Using Vertical Wells at the Portsmouth Gaseous Diffusion Plant, EPA 625-R-99-012, pp. 42-49

Marvin, B.K., Chambers, J., Leavitt, A., and Schreier, C.G., (2002) Chemical and Engineering Challenges to In Situ Permanganate Remediation, Battelle Press, Monterey, CA, pp. 1127-1134

McDonald, M.G., and Harbaugh, A.W., (1988) A Modular Three-Dimensional Finite-Difference Ground-Water Flow Model, *Techniques of Water-Resources Investigations*, Book 6, US Geological Survey, pg. 586

Mumford, K.G., Thomson, N.R., and Allen-King, R.M., (2002) Investigating the Kinetic Nature of Natural Oxidant Demand During ISCO, Battelle Press, Monterey, CA, pp. 1383-1388

Mumford, K.G., Lamarche, C.S., and Thomson, N.R., (2004) Natural Oxidant Demand of Aquifer Materials Using the Push-Pull Technique, *Journal of Environmental Engineering* 130(10), pp. 1139-1146

Mumford, K.G., Thomson, N.R., and Allen-King, R.M., (2005) Bench-Scale Investigation of Permanganate Natural Oxidant Demand Kinetics, *Environmental Science and Technology* 39(8), pp. 2835-2840

Oberle, D.W., and Schroder, D.L., (2000) Design Considerations for In-Situ Chemical Oxidation, *Chemical Oxidation and Reactive Barriers; Remediation of Chlorinated and Recalcitrant Compounds*, pp. 91-99

Reitsma, S., and Dai, Q.L., (2001) Reaction-Enhanced Mass Transfer and Transport from Non-Aqueous Phase Liquid Source Zones, *Journal of Contaminant Hydrology* 49(1-2), pp. 49-66

Schnarr, M., Truax, C., Farquhar, G., Hood, E., Gonullu, T., and Stickney, B., (1998) Laboratory and Controlled Field Experiments Using Potassium Permanganate to Remediate Trichloroethylene and Perchloroethylene DNAPLs in Porous Media, *Journal of Contaminant Hydrology* 29(3), pp. 205-224

Siegrist, R.L., Lowe, K.S., Murdoch, L.D., Slack, W.W., and Houk, T.C., (1998a) X-231A Demonstration of In Situ Remediation of DNAPL Compounds in Low Permeability Media by Soil Fracturing with Thermally Enhanced Mass Recovery or Reactive Barrier Destruction, Oak Ridge National Laboratory Report, ORNL/TM-13534

Siegrist, R.L., Lowe K.S., Murdoch, L.C., Case, T.L., Pickering, D.A., and Houk, T.C., (1998b) Horizontal Treatment Barriers of Fracture-Emplaced Iron and Permanganate Particles, EPA 542-R-98-003, pp. 77-83

Siegrist, R.L., Urynowicz, M.A., and West, O.R., (2000) An Overview of In Situ Chemical Oxidation Technology Features and Applications, EPA 625-R-99-012, pp. 61-69

Siegrist, R.L., Urynowicz, M.A., West, O.R., Crimi, M.L., and Lowe, K.S., (2001) Principles and Practices of In Situ Chemical Oxidation Using Permanganate, Battelle Press, Columbus, OH

Steel, E.W., and McGhee, T.J., (1979) *Water Supply and Sewerage*, Fifth Edition, McGraw-Hill, New York, NY

Tompson, A.F.B., Aboudu, R., and Gelhar L.W., (1989) Implementation of the Three Dimensional Turning Bands Random Field Generator, *Water Resources Research* 25(10), pp. 2227-2243

US EPA, (1998) *Field Applications of In Situ Remediation Technologies: Chemical Oxidation*, US Environmental Protection Agency, Solid Waste and Emergency Response, EPA 542-R-98-008

US EPA, (2007) *Treatment Technologies for Site Cleanup: Annual Status Report (Twelfth edition)*, US Environmental Protection Agency, Solid Waste and Emergency Response, EPA 542-R-07-012

Urynowicz, M.A., Balu, B., and Udayasankar, U., (2008) Kinetics of Natural Oxidant Demand by Permanganate in Aquifer Solids. *Journal of Contaminant Hydrology* 96(1-4), pp. 187-194

Vella, P.A., Deshinsky, G., Boll, J.E., Munder, J., and Joyce, W.M., (1990) Treatment of Low Level Phenols with Potassium Permanganate, *Research Journal of the Water Pollution Control Federation* 62(7), pp. 907-914

Vella, P.A., and Veronda, B., (1992) Oxidation of Trichloroethylene: A Comparison of Potassium Permanganate and Fenton's Reagent, In: *Proceedings of the Third International Symposium on Chemical Oxidation Technology for the Nineties*, Vanderbilt University, Nashville, TN

West, O.R., Cline, S.R., Holden, W.L., Gardner, F.G., and Schlosser, B.M., (1998) Field-scale Test of In Situ Chemical Oxidation through Recirculation, In: *Proceedings of Spectrum '98 International conference on Nuclear and Hazardous Waste Management*, Denver, CO, pp. 1051-1057

Water Science and Technology Board (WSTC), (2004) *Contaminants in the Subsurface: Source Zone Assessment and Remediation*, Division on Earth and Life Studies, National Research Council of the National Academies, THE NATIONAL ACADEMIES PRESS, Washington DC

Xu, X., (2006) *Interaction of Chemical Oxidants with Aquifer Materials*, Civil and Environmental Engineering, Waterloo, University of Waterloo, PhD Dissertation

Yan, Y.E., and Schwartz F.W., (1996) *Oxidation of Chlorinated Solvents by Permanganate, Physical, Chemical, and Thermal Technologies: Oxidation Technologies*, G.B. Wickramanayake and R. E. Hinclee eds, Battelle Press, pp. 403-408

Yan, Y.E., and Schwartz, F.W., (1999) Oxidative Degradation and Kinetics of Chlorinated Ethylenes by Potassium Permanganate, *Journal of Contaminant Hydrology* 37(3), pp. 343-365

Zhang, H., and Schwartz, F.W., (2000) Simulating the In Situ Oxidative Treatment of Chlorinated Ethylenes by Potassium Permanganate, *Water Resources Research* 36(10), pp. 3031-3042

APPENDIX

APPENDIX A MODEL VALIDATION

A.1 Analytical Solution

The RT3D reaction module was verified against an analytical solution for both decay and no decay cases. The 1-D analytical solution for solute transport (A-1) with first order decay (Bear, 1972) is

$$C(x,t) = \frac{C_0}{2} \exp\left[\frac{v_x x}{2D_h}\right] \cdot \left[\exp(-x\beta) \cdot \operatorname{erfc}\left(\frac{x - [v_x^2 + 4\lambda D_h]^{1/2} t}{2[D_h t]^{1/2}}\right) + \exp(\beta x) \cdot \operatorname{erfc}\left(\frac{x + [v_x^2 + 4\lambda D_h]^{1/2} t}{2[D_h t]^{1/2}}\right) \right] \quad (\text{A-1})$$

where, $\beta^2 = \frac{v_x^2}{4D_h^2} + \frac{\lambda}{D_h}$, and v_x is seepage velocity, D_h is the numerical

dispersion coefficient, λ is the 1st order decay rate, C_0 is the initial concentration of species, x is the distance from source location, and t is the time.

Since kinetic relationship (Model 6) use 2nd order reaction rate (k_{2s}), λ need to be extracted from below equation (A-2).

$$\frac{dM}{dt} = -\rho_B k_{2s} N_s M / n \quad (\text{A-2})$$

When slow NOD (N_s) is much greater than permanganate, N_s will remain essentially constant.

$$N_s \gg M \rightarrow N_s \approx \text{constant} \quad (\text{A-3})$$

then, λ is calculated from equation (A-4).

$$\lambda = \rho_B k_{2s} N_s / n \quad (\text{A-4})$$

Below **Table A-1** show the parameters used for analytical solution.

Table A-1 Parameters for Analytical Solution

| | |
|--|------------------------------|
| Permanganate Concentration (C_0) | 250 mol/L |
| seepage velocity (v_x) | 0.505051 m/day |
| Length of Model (x) | 9.9 m |
| Numerical dispersion coefficient(D_h) | 0.505051 m ² /day |
| 1 st order decay rate (λ) | .005 day ⁻¹ |
| NODs | 5000 mol/Kg |
| Porosity | 0.2 |
| Bulk density | 2 kg/L |

A.2 Model Setup

1-D homogeneous system has been setup for comparison of analytical solution and numerical model. Unit area was 1m² and length of model was 10m with $\Delta x = 0.1$ m. Hydraulic gradient (i) was 1m/9.9m = 0.10101 from center of up-gradient cell to down-gradient cell and permeability was used 1m/day. Porosity was 0.2 and bulk density was 2 kg/L for entire model. Slow NOD reaction rate was used arbitrary value of 10E-06 L/mol-day. The parameters used for model are listed in **Table A-2**. These parameters result in an effective first order decay rate for M of 0.005 per day.

Table A-2 Parameters for Numerical Analysis

| | |
|---|-----------------|
| Permanganate Concentration | 250 mol/L |
| Head gradient | 0.10101 |
| Length of Model | 9.9 m |
| Longitudinal dispersivity | 1 m |
| 2 nd order decay rate (k_{2s}) | 10E-6 L/mol-day |
| NODs | 5000 mol/Kg |
| Porosity | 0.2 |
| Bulk density | 2 kg/L |

A.3 Comparison and Results

Comparisons are conducted at the end of the model with reactive and non-reactive cases. **Figure A-1** and **A-2** show the result of non-reactive and reactive at 9.9m of the model as well.

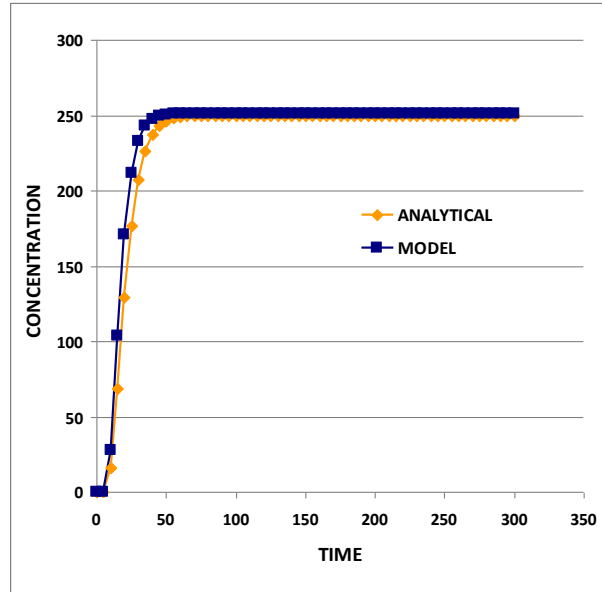


Figure A-1 Comparison of Analytical Solution and Numerical Modeling Result with Non-Reactive at 9.9m of Model.

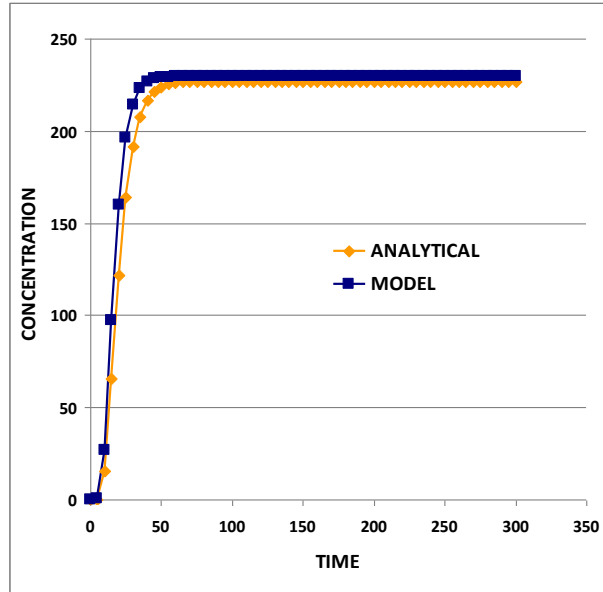


Figure A-2 Comparison of Analytical Solution and Numerical Modeling Result with Reactive at 9.9m of Model.

The final concentration of permanganate at **Figure A-2** was slightly less than initial value of 250 because permanganate consumed by slow NOD. Both of figures show the well matched result between analytical solution and numerical modeling. Root mean square error (RMSE) was 9.5 for non-reactive, 9.1 for reactive case. Dividing initial permanganate concentration gives 3.6 ~3.8 of error percent between analytical solution and numerical modeling.